NAVAL POSTGRADUATE SCHOOL
Monterey, California

THESIS

DESIGN AND COST-BENEFIT ANALYSIS OF A MINI THERMO-ACOUSTIC REFRIGERATOR DRIVER

by

Omer Livvarcin

September 2000

Thesis Advisor: Thomas J. Hofler
Thesis Advisor: Roger Evered

Approved for public release; distribution is unlimited.

REPORT DOCUMENTATION PAGE

Form Approved
OMB No. 0704-0188

1. AGENCY USE ONLY *(Leave blank)*	2. REPORT DATE	3. REPORT TYPE AND DATES COVERED
	September 2000	Master's Thesis

4. TITLE AND SUBTITLE
Design And Cost-Benefit Analysis Of A Mini Thermo-Acoustic Refrigerator Driver

5. FUNDING NUMBERS

6. AUTHOR(S)
Livvarcin, Omer

7. PERFORMING ORGANIZATION NAME(S) AND ADDRESS(ES)
Naval Postgraduate School
Monterey, CA 93943-5000

8. PERFORMING ORGANIZATION REPORT NUMBER

9. SPONSORING / MONITORING AGENCY NAME(S) AND ADDRESS(ES)

10. SPONSORING / MONITORING AGENCY REPORT NUMBER

11. SUPPLEMENTARY NOTES
The views expressed in this thesis are those of the author and do not reflect the official policy or position of the Department of Defense or the U.S. Government.

12a. DISTRIBUTION / AVAILABILITY STATEMENT
Approved for public release; distribution is unlimited.

12b. DISTRIBUTION CODE

13. ABSTRACT *(maximum 200 words)*

A miniature thermoacoustic refrigerator is being developed for the purpose of cooling integrated circuits below their failure temperature when used in hot environments. This thesis describes the development of an electrically powered acoustic driver that powers the thermoacoustic refrigerator. The driver utilizes a flexural tri-laminar piezoelectric disk to generate one to two Watts of acoustic power at 4 kHz in 15 bar of He-Kr gas mixture.

This thesis also provides a cost analysis of the mini TAR and a comparison with other cooling methods in terms of cost and benefits. It estimates the unit cost of a Mini TAR and compares it with other existing microchip coolers in terms of cost and benefits.

14. SUBJECT TERMS	15. NUMBER OF PAGES
thermoacoustic refrigerator, TAR, thermo-acoustic driver, cost analysis, microchip cooling	122
	16. PRICE CODE

17. SECURITY CLASSIFICATION OF REPORT	18. SECURITY CLASSIFICATION OF THIS PAGE	19. SECURITY CLASSIFI- CATION OF ABSTRACT	20. LIMITATION OF ABSTRACT
Unclassified	Unclassified	Unclassified	UL

NSN 7540-01-280-5500

Standard Form 298 (Rev. 2-89)
Prescribed by ANSI Std. 239-18

Approved for public release; distribution is unlimited

DESIGN AND COST-BENEFIT ANALYSIS OF A MINI THERMO-ACOUSTIC REFRIGERATOR DRIVER

Omer Livvarcin
LTJG, Turkish Navy
B.A., Turkish Naval Academy, Istanbul, 1994

Submitted in partial fulfilment of the
requirements for the degree of

MASTER OF SCIENCE IN ENGINEERING ACOUSTICS
AND
MASTER OF SCIENCE IN SYSTEMS MANAGEMENT

from the

NAVAL POSTGRADUATE SCHOOL
September 2000

Author: _____
Omer Livvarcin

Approved by: _____
Thomas J. Hofler, Thesis Advisor

_____
Roger Evered, Thesis Advisor

_____
Reuben T. Harris, Chairman,
Department of Systems Management

_____
Kevin Smith, Chairman,
Engineering Acoustics Academic Committee

ABSTRACT

A miniature thermoacoustic refrigerator is being developed for the purpose of cooling integrated circuits below their failure temperature when used in hot environments. This thesis describes the development of an electrically powered acoustic driver that powers the thermoacoustic refrigerator. The driver utilizes a flexural tri-laminar piezoelectric disk to generate one to two Watts of acoustic power at 4 kHz in 15 bar of He-Kr gas mixture.

This thesis also provides a cost analysis of the mini TAR and a comparison with other cooling methods in terms of cost and benefits. It estimates the unit cost of a Mini TAR and compares it with other existing microchip coolers in terms of cost and benefits.

TABLE OF CONTENTS

ACKNOWLEDGEMENTS

I would like to thank Professor Hofler and Professor Evered for their instructions, assistance and patient guidance during this thesis project. My thanks also go to my colleagues, Aaron Chia and Seyhmus Direk for their assistance. Special gratitude to my parents, Necmiye and Asim Livvarcin for supporting me the whole of my life. And finally, a very special thank you to my wonderful wife, Serap Livvarcin, for being there whenever I needed her and for being so patient during my difficult days.

I. INTRODUCTION

Thermoacoustic refrigeration is a technological advance that provides improved cooling capacity without the need for environmentally destructive refrigerants such as chlorofluorocarbons. The basic mechanism of the thermoacoustic refrigerator (TAR) is very simple yet efficient, and is based on the expansion and compression of a gas in the form of a sound wave.

A sound wave is really nothing more than a periodic compression and expansion of a gas along with small gas motions. When a sound wave from a vibrating diaphragm or a loudspeaker is sent down a hollow, half-wavelength tube, the pressure pulsations make the gas inside slosh back and forth. Because gas becomes warmer as it is compressed and cools as it expands, this movement forms regions where compression and heating take place as well as expansion and cooling. In this manner, a sound wave heats and cools small parcels of gas along the length of its propagation.

A. OBJECTIVE

The goal of this thesis project is to design and build a mini TAR for micro-electronic "chip" cooling using a custom piezoelectric driver built with components taken from Motorola tweeters. This mini TAR is intended to

eventually surpass the current levels of efficiency and durability of existing thermoelectric coolers.

This thesis will also provide a cost analysis of the mini TAR and a comparison with other cooling methods in terms of cost and efficiency. This thesis will answer the question about the estimated unit cost of a Mini TAR and give us the opportunity to compare it with other existing microchip coolers in terms of cost and efficiency. All this information about the costs and benefits of the Mini TAR will help decision makers to make the right decision depending on their requirements.

B. THESIS ORGANIZATION

Chapter II provides a basic foundation for the development and current applications of TAR's and piezoelectric devices. This chapter gives information about thermoacoustic principles.

Chapter III describes the thermoacoustic requirements for the mini TAR driver. Since this project is sponsored by Rockwell, some of the requirements are defined by that company.

Chapter IV details the measurements of the Motorola piezo driver. These measurements are mostly displacement measurements of the piezo disk under different loading circumstances.

Chapter V shows the design of a simple plastic prototype of a mini TAR. This chapter also includes some performance measurements of the plastic mini TAR.

Chapter VI gives technical information about the design of the mini TAR. Some of the information is obtained by using the DSTAR computer program.

Chapter VII explains in detail the assembly of the mini TAR. Since this thesis will also be used by Rockwell scientists who may need detailed information about the assembly, Chapter VI is written in detail.

In Chapter VIII, the performance measurements and the calibrations of the mini TAR are discussed. This chapter also compares the initial requirements for the mini TAR with the achieved values such as cooling power or the actual cooling performance.

Chapter IX provides a guide and shows some details for the cost analysis of the mini TAR. With the help of some cost data and assumptions where data is not available an estimation of the cost of a unit Mini TAR is also calculated in this chapter.

Cost estimation is the first part of the cost analysis. An efficiency analysis and comparison with other possible microchip cooling methods are the following parts of the cost analysis, and are also explained in this chapter IX.

In concluding the thesis, Chapter X offers general observations and recommendations for the proposed mini TAR model, as well as suggestions for future research and development.

II. BACKGROUND

A. THERMOACOUSTIC HEAT ENGINES

Thermoacoustic engines are classified as heat pumps or prime movers. A thermoacoustic heat pump uses a finite-amplitude standing acoustic wave to transport thermal energy incrementally along a thermoacoustic "stack" from one heat exchanger to another. The acoustically generated heat transfer produces a significant thermal gradient over the length of the stack. This conversion of acoustic energy into stored thermal energy can be used for a wide variety of diverse applications, including refrigeration.

This process followed in a reverse order closely resembles the workings of a thermoacoustic prime mover, in which stored thermal energy from an external source is converted into kinetic energy in the form of acoustic waves. The conversion of energy occurs when heat delivered by a heat exchanger causes a temperature differential of sufficient magnitude over the length of a stack, causing in turn an acoustic instability to occur in the internal gas. This instability has an initial exponential rise in amplitude with a growth rate that increases with the temperature gradient. and a frequency given by the natural resonance, (e.g., the resonance may be determined by a quarter wavelength tube resonance.) After the initial exponential growth, the

amplitude will reach a limit determined by the complex nonlinear interplay between heat-exchanger conduction, acoustic dissipation and loading characteristics.

The primary attraction of thermoacoustic heat engines is that they can be constructed in a range of sizes, allowing for a large variety of applications, and have few or no moving components. When compared to conventional heat engines, they are extremely simple and inherently reliable, and also feature another significant benefit in that they do not require chlorofluorocarbons (CFC's) or other environmentally damaging substances.

B. THERMOACOUSTIC PROCESS

A complete analytical analysis of the thermoacoustic process is provided by Swift [Ref. 1,3], and is used as the basis for the following description.

1. Efficiency and The Carnot Cycle

All reversible heat engines operate in one of two modes -- as a prime mover or as a heat pump. As a prime mover, the application of thermal energy from two reservoirs of differing temperature will generate useful work within the engine. As a heat pump, the application of work to the engine will

cause heat energy to flow from a region of lower temperature to one of higher temperature.

The First and Second Laws of Thermodynamics place a limit on the efficiency of any process involving the use of heat engines. This limit depends solely on the temperatures of the two reservoirs used by the heat engine, the high temperature reservoir with a temperature of Th, and the cold reservoir with a temperature of Tc. The flows of associated heat energy into and out of the heat engine are given as the heat flow to or from the hot reservoir, Qh, and to or from the cold reservoir, Qc. The resulting work is expressed by the symbol W.

The First Law of Thermodynamics states that for any process, the total energy of the system must be conserved, i.e.,

$$Q_h - Q_c = W \tag{2.1}$$

The Second Law of Thermodynamics states that the total entropy generated by any real process must be positive or zero. Understanding that entropy can be expressed as proportional to the heat flow to a reservoir divided by the temperature of that reservoir, the 2nd Law can be expressed as:

$$\frac{Q_c}{T_c} - \frac{Q_h}{T_h} \geq 0 \quad \text{(Prime Mover)} \tag{2.2}$$

or

$$\frac{Q_h}{T_h} - \frac{Q_c}{T_c} \geq 0 \quad \text{(Heat Pump)} \tag{2.3}$$

For the case of a prime mover, the efficiency is,

$$\eta = \frac{W}{Q_h} \tag{2.4}$$

which, when combined with equations (2.1) and (2.4) reduces to

$$\eta \leq \frac{T_h - T_c}{T_h} \tag{2.5}$$

The Carnot efficiency represents the upper bound that any prime mover can achieve.

In the case of an engine operating as a heat pump, the power performance is referred to as the *Coefficient of Performance* (COP), and is given by:

$$COP = \frac{Q_c}{W} \tag{2.6}$$

which, when combined with equations (2.1) and (2.6), reduces to

$$COP_c \leq \frac{T_c}{T_h - T_c} \tag{2.7}$$

The Carnot Coefficient of Performance represents the upper bound for the COP for any heat pump. The Carnot Cycle, as shown in Figure 2.1, represents the ideal thermodynamic cycle in which the net increase in entropy over the cycle is zero.

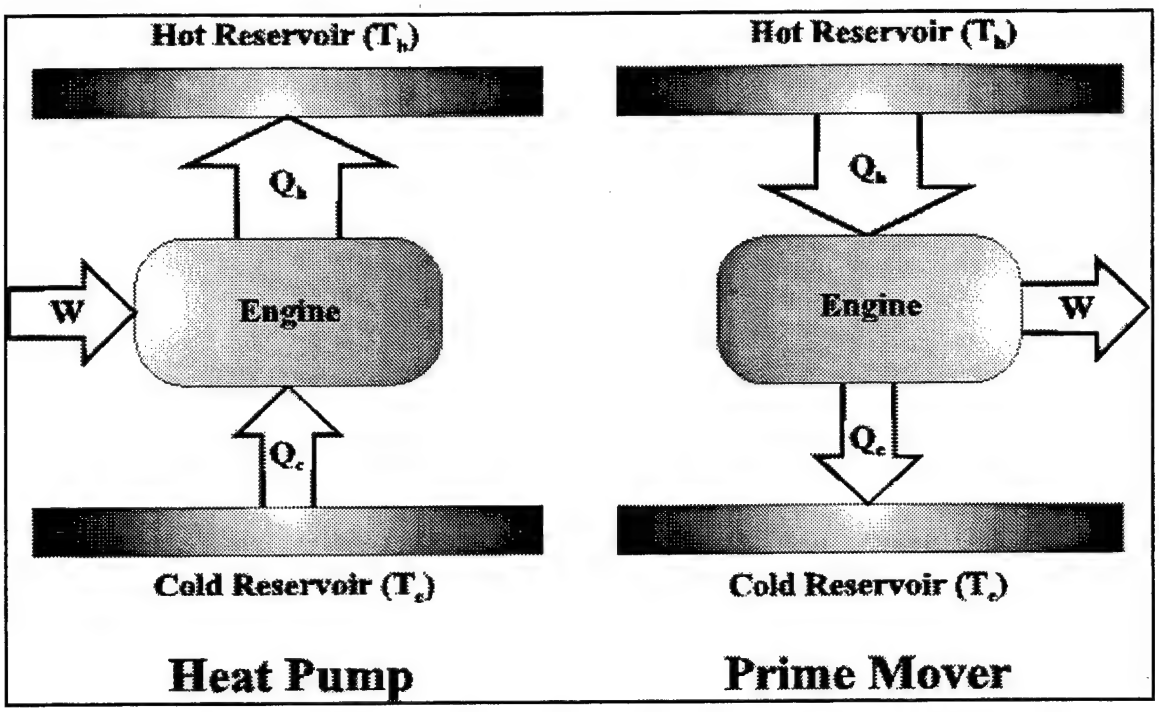

Figure 2.1. Heat Engine Operation

For this ideal cycle, there are two isothermal steps in which work and heat flow into or out of the engine, and two adiabatic steps in which compression and expansion of the fluid medium occurs. When carried out at near equilibrium conditions, the total increase in the entropy of the system during the expansion step is exactly equal to the total drop in the entropy during the compression step. Any real thermodynamic engine generating useful work will not operate under these conditions, and will therefore have a net increase in the total entropy over one cycle. It is for this reason that the Carnot Cycle represents the upper bound of the possible efficiency of any heat engine, be it a prime mover or a heat pump.

The Carnot Cycle

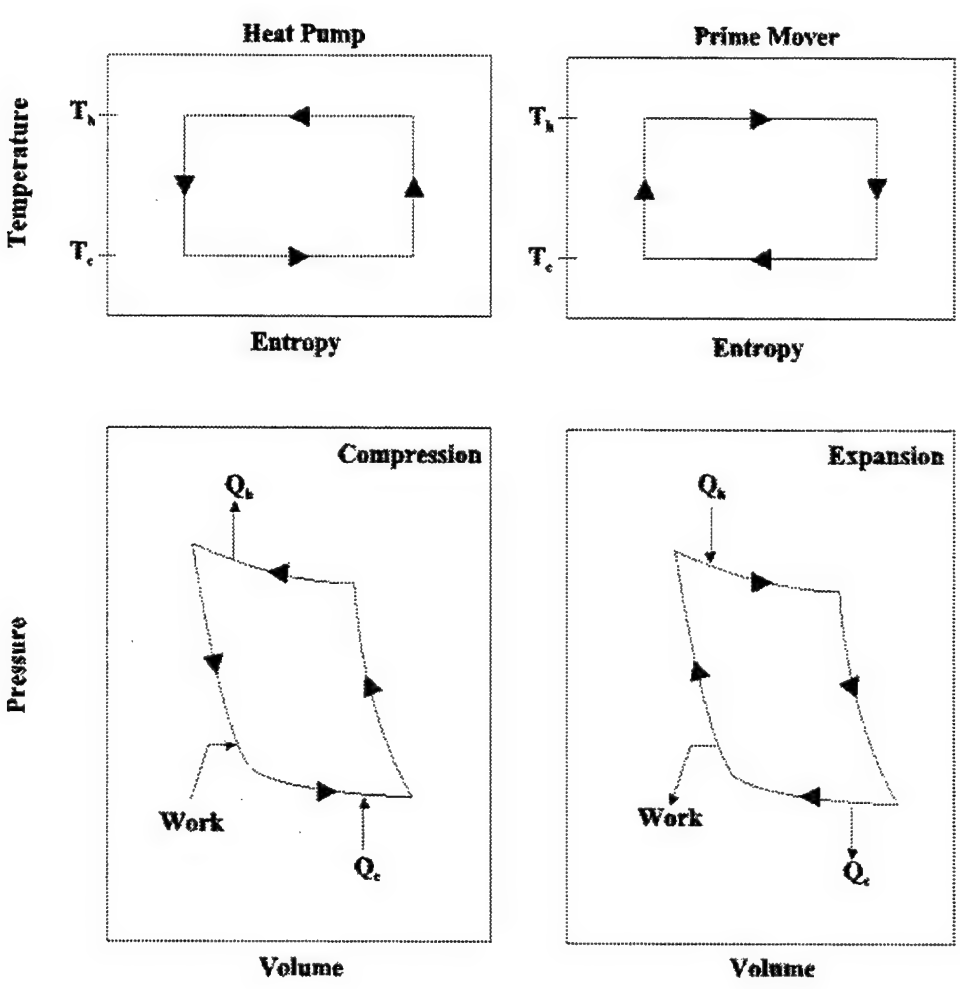

Figure 2.2. The Carnot Cycle temperature-entropy (T-S) and Pressure-Volume (P-V) diagrams for both the prime mover and heat pump. The near equilibrium state of the cycle ensures that the total change in entropy over one cycle is zero. This yields the rectangular plot in the T-S diagram, and ensures that the total work added to or removed from the engine is equal to the area enclosed by the P-V cycle.

C. THERMOACOUSTIC ENGINES

1. Engine Design

A thermoacoustic engine converts thermal energy from a high temperature heat source into useful work, in the form of acoustic power, while diverting waste thermal energy into a cold heat sink. To accomplish this task, several components are required. The first is a means for the high thermal energy to enter the engine. This is referred to as the hot heat exchanger. Second, a means of expelling waste thermal energy from the engine to the cooler heat sink is required. This is called the cold heat exchanger.

Between the two heat exchangers is a set of precisely spaced metal plates referred to as the stack. The purpose of the stack is to provide a means of temporary heat storage and to provide a smooth temperature gradient from the hot heat exchanger to the cold heat exchanger.

The final basic component, and the most important factor in determining the operation of the engine, is the resonator tube. This tube determines the frequency of the acoustic energy produced by the engine.

In an open tube configuration, as shown in Figure 2.3, the lowest resonant mode is a quarter wavelength with pressure anti-nodes at the closed end and pressure nodes at the open end. This configuration ensures that the

fundamental will have a wavelength approximately four times the length of the tube. Other configurations are possible, including a closed end resonator with pressure nodes at both ends producing acoustic power at a wavelength two times the physical length of the tube.

2. Thermoacoustic Requirements and the Thermodynamic Cycle

To gain a qualitative understanding of a thermoacoustic heat engine's operation, the Lagrangian approach is best adopted, and entails following a finite parcel of the gas to demonstrate the thermoacoustic effect.

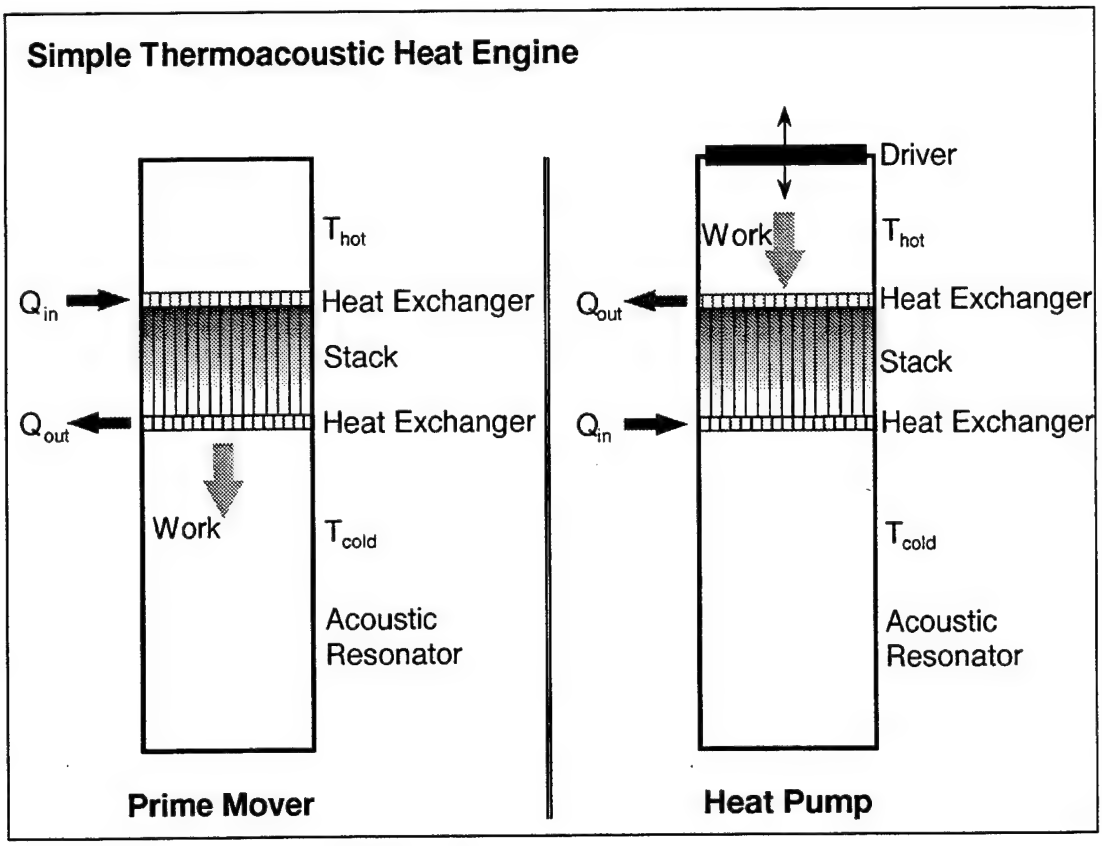

Figure 2.3. Simple Thermoacoustic Engine (from Purdy [Ref. 2])

Although the acoustic oscillations within the resonator are sinusoidal, the cycle is best explained by approximating the sinusoid with a square wave. The cycle then consists of two reversible adiabatic steps and two irreversible constant pressure steps, identical to the conventional Brayton cycle [Ref. 4].

In a conventional heat engine, coordinated crankshafts and camshafts mechanically control piston movement and valve actuation. In a thermoacoustic heat engine, there are no mechanical elements to ensure the

proper phasing of the cycle. The key to phasing within a thermoacoustic heat engine is the presence of two thermodynamic media, the fluid and the stack plate.

The change in the temperature of the gas parcel as it moves along the plate comes from the adiabatic compression and expansion of the parcel and from the presence of the plate that is operating at a different temperature than the gas parcel. The heat flow between the gas parcel and the plate does not produce an instantaneous change in temperature, but there is a time delay between the temperature and pressure. To ensure that this time delay is correct, a specific thermal conductivity is required.

If the thermal conductivity is too high, the change in temperature of the gas parcel will occur too rapidly, and therefore no time delay will be created. If the thermal conductivity is too small, no appreciable temperature change will occur and the cycle will not be driven. The proper thermal conductivity is related to the thermal penetration depth, δ_κ. The thermal penetration depth is the distance heat diffuses through the fluid medium during a time $1/\delta_\kappa$, and is defined by

$$\delta_\kappa = \sqrt{\frac{2\kappa}{\omega}} \tag{2.8}$$

where κ is the fluid's thermal diffusivity [Ref. 1].

A rough analysis has shown that the optimal spacing of the plates within a stack is approximately 4 δ_κ. Detailed optimization of this parameter will generally result in variations as large as a factor of two, depending on the type of thermoacoustic engine being designed and its temperature range.

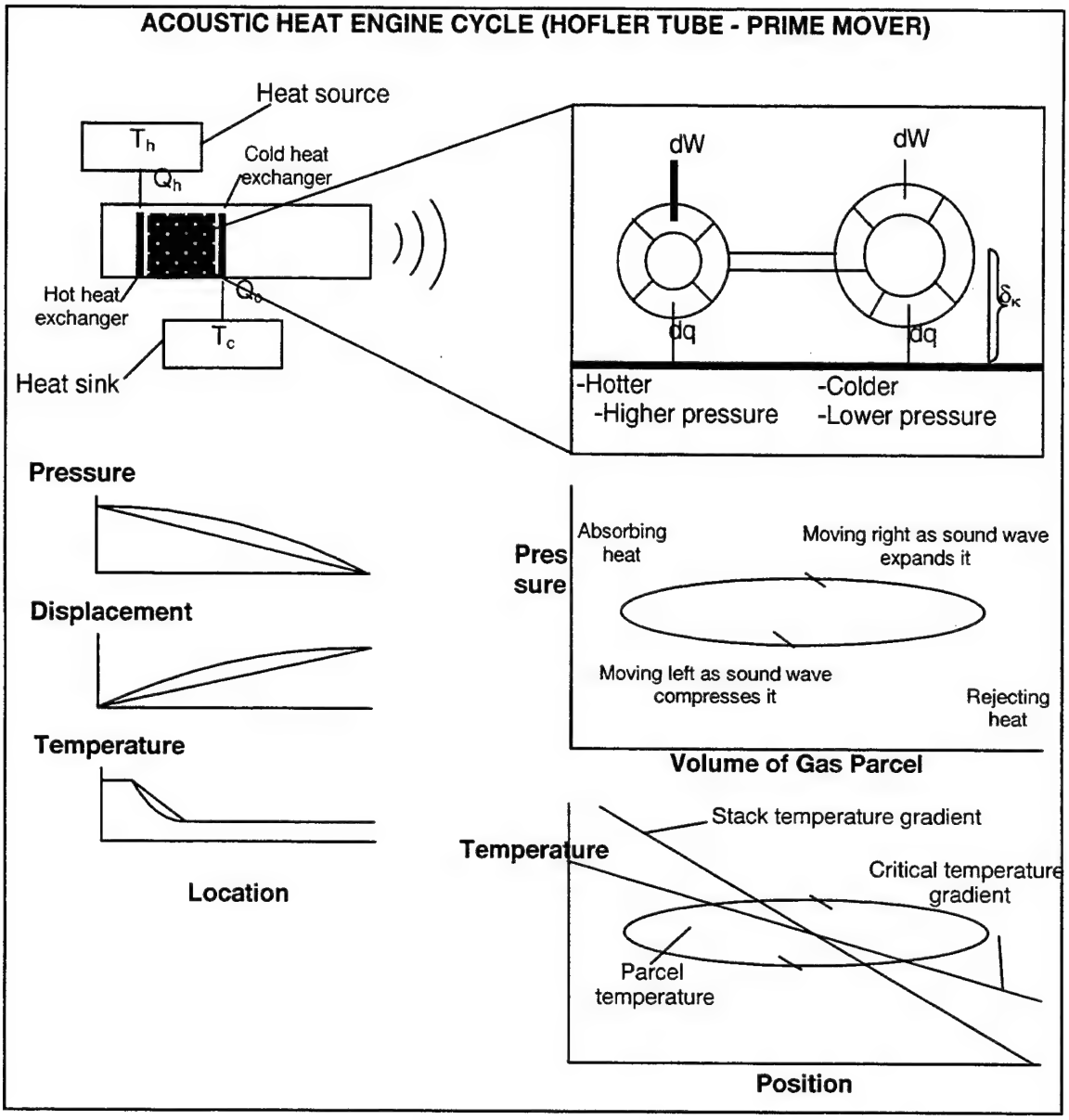

Figure 2.4.The Thermoacoustic Cycle: Shown is the cycle undergone by one infinitesimal parcel of gas. (a) The parcel adiabatically expands and moves to the right, away from the increasing acoustic pressure. (b) The parcel rejects heat energy to the cooler stack plating. (c) The oscillating acoustic pressure compresses the parcel and drives it back to the left. (d) The parcel absorbs heat energy from the hot stack plate [Ref. 1].

Figure 2.4. shows the movement, heat transfer, and volume changes of a parcel of gas as it moves during one cycle. Initially, the gas parcel is

stationed at one thermal penetration depth from the plate in a region of high acoustic pressure gradient. The high-pressure gradient drives the parcel to the right, while at the same time the parcel absorbs heat from the plate. The combination of the decreasing acoustic pressure and the increasing temperature of the parcel causes its volume to increase during the movement to the right. As the parcel moves toward the cooler portion of the stack plating, it begins to release heat energy into the plate. The oscillating acoustic pressure creates a region of reverse high-pressure gradient at this point, driving the parcel back to the left toward the region of high temperature while at the same time compressing the parcel.

Once the parcel returns to the initial point at which the cycle began, it is in its initial state and begins the cycle again. Each iteration of the cycle causes a small amount of heat energy to be transferred from the region of high temperature to the region of low temperature. In the next section, it will be shown how this effect can be exploited to create useful thermoacoustic engines, whether operating as a prime mover or as a heat pump.

3. The Rott Wave and Energy Flow Equations

Advancement beyond a basic qualitative description of the theory of thermoacoustic heat engines to a quantitative description requires the Rott equations. (The derivation of these equations is provided by [Ref. 5], and due

to their length and complexity, will not be presented here.) These equations, as modified by Swift, form the foundation of numerical models of thermoacoustic devices such as DSTAR.

Rott developed the first equation for acoustic propagation within a channel formed by parallel plates, where the plates may have a temperature gradient. This equation, modified by Swift, serves to describe the acoustic wave within the stack, which is closely approximated by such a channel [Ref. 3], and is given by

$$\left(1+\frac{(\gamma-1)f_\kappa}{1+\varepsilon_s}\right)p_1+\frac{\rho_m a^2}{\omega^2}\frac{d}{dx}\left(\frac{1-f_\nu}{\rho_m}\frac{dp_1}{dx}\right)-\beta\frac{a^2}{\omega^2}\frac{f_\kappa-f_\nu}{(1-\sigma)(1+\varepsilon_s)}\frac{dT_m}{dx}\frac{dp_1}{dx}=0 \quad (2.10)$$

where

$$f_\nu=\frac{\tanh[(1+i)y_0/\delta_\nu]}{(1+i)y_0/\delta_\nu}$$

$$f_\kappa=\frac{\tanh[(1+i)y_0/\delta_\kappa]}{(1+i)y_0/\delta_\kappa}$$

$$\varepsilon_s=\frac{\sqrt{K\rho_m c_p}\tanh[(1+i)y_o/\delta_\kappa]}{\sqrt{K_s\rho_s c_s}\tanh[(1+i)y_o/\delta_s]}$$

$$\sigma=c_p\mu/K=\nu/\kappa$$

$$\delta_\kappa=\sqrt{2\kappa/\omega}$$

$$\delta_\nu=\sqrt{2\nu/\omega}$$

The above equation is a general form that is applicable for both liquids and gases as the propagation medium. However, if the medium is assumed to be an ideal gas, the ideal gas law may be applied. This, combined with the

definition of a set of non-dimensional state variables, reduces Equation (2.7) to [Ref. 3,5]

$$\left[1+\frac{(\lambda-1)f_\kappa}{1+\varepsilon_s}\right]\mathbf{P}+\left[(1+f_v)+\frac{1}{2}(1+\beta_r)(f_v+\tanh^2\eta_0-1)-\frac{f_\kappa-f_v}{(1-\sigma)(1+\varepsilon_s)}\right]\frac{d\mathbf{T}}{d\mathbf{X}}\frac{d\mathbf{P}}{d\mathbf{X}}+(1-f_v)\mathbf{T}\frac{d^2\mathbf{P}}{d\mathbf{X}^2}=0 \quad (2.11)$$

where

$$\eta_0=(1+j)(y_0/\delta_v)\,. \quad (2.12)$$

The capitalized, bold-faced variables are normalized or non-dimensional variables, and are defined in Appendix A. Equation (2.11) allows the complex state variables of pressure and pressure gradient or velocity to be determined if the temperature gradient is known.

The second parameter of interest for the development of thermoacoustic models is the 2nd order enthalpy, H_2. This energy flow equation, as developed in Ref [5] is

$$\begin{aligned}\dot{H}_2=&\frac{\Pi y_0}{2\omega\rho_m}\mathrm{Im}\left[\frac{d\tilde{p}_1}{dx}p_1\left(1-\tilde{f}_v-\frac{T_m\beta(f_\kappa-\tilde{f}_v)}{(1+\varepsilon_s)(1+\sigma)}\right)\right]\\&+\frac{\Pi y_o c_p}{2\omega^3\rho_m(1-\sigma)}\frac{dT_m}{dx}\frac{dp_1}{dx}\frac{d\tilde{p}_1}{dx}\\&\times\mathrm{Im}\left[\tilde{f}_v+\frac{(f_\kappa-\tilde{f}_v)(1+\varepsilon_s f_v/f_\kappa)}{(1+\varepsilon_s)(1+\sigma)}\right]\\&-\Pi(y_0K+lK_s)\frac{dT_m}{dx}\end{aligned} \quad (2.13)$$

The final local state variable of temperature can be determined by DSTAR with Equation 2.14. If the energy equation is rearranged to express

the temperature derivative with respect to position in terms of the constant energy term and acoustic variables, and an ideal gas law and non-dimensional variables are used, the result is:

$$\frac{d\mathbf{T}}{d\mathbf{X}} = \frac{\mathbf{T}\,\mathrm{Im}\left[\frac{d\tilde{\mathbf{P}}}{d\mathbf{X}}\mathbf{P}\left(1-\tilde{f}_v-\frac{f_\kappa-\tilde{f}_v}{(1+\varepsilon_s)(1+\sigma)}\right)-\mathbf{H}_2\right]}{\frac{\mathbf{T}}{(\lambda-1)(1-\sigma)}\left|\frac{d\mathbf{P}}{d\mathbf{X}}\right|^2\mathrm{Im}\left[1-\tilde{f}_v-\frac{(f_\kappa-\tilde{f}_v)(1+\varepsilon_s f_v/f_\kappa)}{(1+\varepsilon_s)(1+\sigma)}\right]+\mathbf{K}} \tag{2.14}$$

With the development of the wave and energy equations described above, mathematical techniques must be used to determine the solutions applicable to the device of interest. To properly solve the equations as initial value problems or boundary value problems, numerical techniques must be used since closed form solutions are not available.

III. DETERMINATION OF THERMOACOUSTIC REQUIREMENTS FOR A DRIVER

Before designing a mini TAR, performance expectations must be defined. The mini TAR will be designed according to these expectations. All other properties of the mini TAR (e.g., the parameters of the driver, the length of tube or the pressure of the gas in the tube) are all related to the definitions that are related to the performance expectations. With the aid of computer programs, it is possible to calculate the outputs and define thermoacoustic requirements before building hardware.

The Design Simulation for Thermoacoustic Research (DSTAR) computer modeling software can be used to determine the mini TAR's thermoacoustic requirements. DSTAR is a Windows™-compliant graphical based program that provides a flexible and powerful tool for the design and analysis of thermoacoustic heat engines. Further information about DSTAR can be found in Chapter II.

A. THERMOACOUSTIC REQUIREMENTS FOR THE MINI TAR

Rockwell, the corporate sponsor of the mini TAR development project, defined the original performance expectations for the mini TAR. Rockwell envisioned a mini TAR that would operate around 10 kHz, with 1 W cooling

power between 60°C and 90°C, and a 1-inch total length. But due to the difficulties encountered, (i.e., finding a driver with 10 kHz frequency and designing very small components) the performance expectations were subsequently modified. The thesis project's ultimate goal is to design an acoustic driver for a mini TAR with 1 W cooling power (between the temperatures mentioned above) that can operate at around 4 kHz. The length of the prototype is also increased from its original length of 1 inch to 2 inches.

These specifications for the design of the mini TAR are dependent upon other variables such as the type and the pressure of the gas in the tube, the length of the tube, the diameter of the driver and the Po/Pm ratio. The mini TAR model in this thesis requires 15 bars of gas pressure in the tube (a HeKr mixture), 4 kHz operating frequency, a quarter wavelength tube length and a 5% dynamic pressure ratio, P_o/P_m, (or the ratio between the peak dynamic pressure and the pressure of the gas in the tube). Detailed information about these numbers will be given later in this chapter.

B. LOAD CURVE

Engineers determine load curves for amplifiers or transducers to quantify the output amplitude and power variations with respect in the load impedance. In this thesis the load curve is the graph of the delivered force versus displacement or velocity for a piezoelectric tri-laminar flexural disk.

Drawing the load curve enables us to find the optimum loading point where the mechanical power amplitude is at a maximum value. Two points are used to draw the mini TAR's load curve, both at resonance frequency, one for a piezo disk without any load (except for the air resistance in the room), and one for a mass load of m=1.78 g. The following graph shows the load curve for the mini TAR.

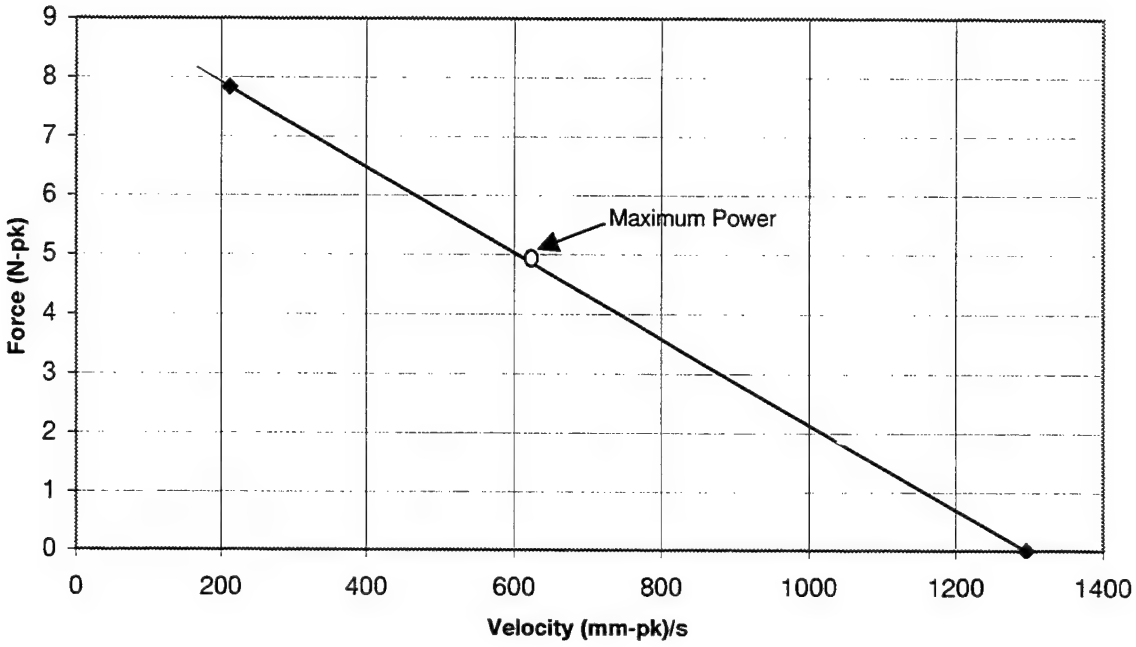

Figure 3.1. Load curve for the mini TAR

Although this load curve is approximate, the graphic representation provides a rough estimate of the optimum point of operation at which mechanical power is at a maximum. This point is shown on the graph with a circle.

For drawing the load curve velocity and forces values are needed. The velocity values are measured with a laser vibrometer. To calculate the force, the following equation is used:

$$F_0 = m\, a_0 \tag{3.1}$$

where,

$$a_0 = \omega\, v_0 \tag{3.2}$$

It is also possible to calculate the mechanical power produced with the vibration of the piezo disk, assuming a resistive load. While no measurements were performed with an actual resistive load, it is hoped that the mass loading results shown in Fig. 3.1 are not dramatically different. The equation for determining mechanical power is as follows:

$$P = \frac{1}{2} F_0 \; v_0 \tag{3.3}$$

According to the graph, the maximum load point is the force is around 4.8 N-pk, where the velocity is approximately 620 mm-pk/s.

Using equation 3.3 to calculate the value of the mechanical power shows that,

$$P = \frac{1}{2} F_0 v_0 = \frac{1}{2} \times 4.8\,N \times 0.62\,m/s = 1.488\,W$$

The value of the power will help to decide whether to use one or two piezo disks for the mini TAR driver. Further information will be given in Chapter 6.

C. DYNAMIC PRESSURE RATIO

The dynamic pressure ratio is the ratio between the peak dynamic pressure and the pressure of the gas in the tube, and can be calculated using the following equation:

$$\text{Dynamic pressure ratio} = \frac{P_0}{P_m} \tag{3.4}$$

In this project, the numerical design model used in DSTAR assumes a dynamic pressure ratio around 5 %.

One other parameter closely related to the dynamic pressure ratio is the pressure of the gas in the tube. The DSTAR model also assumes that the mean pressure of the gas should be 15 bar. Below 15 bar pressure, the total acoustic power will decrease, causing a corresponding drop in the TAR cooling power. Also, lower pressures mean the acoustic penetration depth will increase. Increases in penetration depth increase the acoustic dissipation in the resonator. Mean pressures much higher than 15 bar will make the acoustic penetration depth too small which would exceed our ability to

fabricate the requisite thermoacoustic stack. The fine internal structure of the thermoacoustic stack must match the size of the penetration depth.

A further analysis about cooling power and the performance of the mini TAR can be found in further chapters. The following chapter includes pre-design experiments about the displacement of the piezo disks.

THIS PAGE INTENTIONALLY LEFT BLANK

IV. MEASUREMENTS OF MOTOROLA PIEZO DRIVER

A Thermoacoustic Refrigerator (TAR) is a resonator cavity that contains a stack of thermal storage elements. These elements are connected to hot and cold heat exchangers and same elements are positioned so that back-and-forth gas motion occurs within the stack.

The gas parcels oscillate in temperature because of the acoustic pressure oscillation, in addition to oscillating in position. Because of the temperature oscillation, the moving gas parcels pick up heat from the stack and deposit this heat at a different location in the stack. Similar to the basic principles of a refrigerator's cooling system, the stack acts like a bucket brigade to remove heat from the cold heat exchanger, and then deposit the heat at the hot heat exchange. When the hot heat exchanger gets hotter, the cold heat exchanger at the other end of the stack gets colder which is the underlying principle behind a refrigeration unit. If the hot heat exchange is effective, the heat will be removed from the system without increasing the hot temperature very much.

As previously mentioned, an acoustic driver is needed to create the acoustic standing wave in the stack. The acoustic driver's energy source may be heat, electricity, solar power, or any other source of energy. In this project, electrically driven transducers are used because it is easier to control, acquire

and use electrically driven transducers. Also, the intended application is to cool one or more integrated circuits in an instrument box.

Thermoacoustic refrigeration is a relatively new technology. The prototypes produced thus far are cumbersome, expensive and have only modest efficiency. This thesis aims to build a driver for a miniature TAR (mini TAR) that is expected to be more compact, energy efficient and cheaper.

A. INTRODUCTION TO MEASUREMENTS

Specific measurements must be made prior to designing the prototype mini TAR. These measurements will specify the size, efficiency and capabilities of the prototype.

The first measurements presented in this chapter are the displacement amplitudes of the piezo disk. Additionally, a description of the maximum displacement will provide information about the resonance frequency of the resonance frequency of the transducer.

Using the displacement amplitude measurements is not the only approach to find the resonance frequency. Another method in which electrical impedance and capacitance values are used for the determination of the resonance frequency and the measurements of impedance will be discussed later in this chapter.

Cooling measurements for plastic prototype miniTAR and measurements of damaging input voltages are also covered in this chapter.

B. DISPLACEMENT MEASUREMENTS

The acoustic driver is composed of piezo disks as mentioned in Chapter II. Displacement is the vertical departure of the center of the piezo disk from its initial position as shown in the following figure.

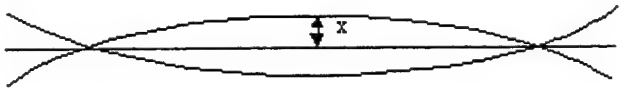

Figure 4.1. The displacement of the piezo disk

Displacement measurement is critical in understanding the driver's behaviors. By knowing the size of the displacement and generated force, it is possible to measure the pressure and the power produced by the driver or the volume velocity of the gas in the tube.

Displacement is expected to be roughly proportional to the driver's input voltage, at least at lower voltages. A sinusoidal A/C input voltage drives the acoustic driver, and the displacement response should also be sinusoidal at the lower voltages. For displacement measurements two types of device are used; the laser vibrometer and the fiber-optic sensor.

Displacement measurements with the laser vibrometer are explained below. The displacement measurements made by the fiber-optic sensor will be explained later in this chapter.

The laser vibrometer is a measuring instrument, which provides velocity information. To obtain the displacement information, the following equation is used:

$$x = \frac{1}{\omega} v_0 \tag{4.1}$$

where v_0 is the peak amplitude of velocity and $\omega = 2\pi f$.

The acceleration of the piezo disk can also be calculated by using the following equation:

$$a_0 = \omega v_0 \tag{4.2}$$

It has been mentioned that the displacement is a result of the input voltage applied to the driver. It is therefore logical to rationalize that the cooling performance of the miniTAR is related to the input voltage of the acoustic driver. Normally, higher input voltage means higher displacement value and better cooling power. However, because of the physical limits of piezoelectric disks, input voltage is limited. Input voltages that exceed the disks' input limitations will damage the piezoelectric disks. Detailed information will be provided later in this chapter about the input voltage limits and the extent of the damage of higher voltages on the disk.

To protect the piezo disk, in this thesis the driver input voltage is limited to 15 Vrms for the prescribed displacement measurement.

The purpose of the displacement measurement is to determine the relationship between the input voltage applied to the acoustic driver and the displacement of the piezoelectric disk.

Also, during the measurements, the driving frequency remains constant at a specific resonance frequency (4120 Hz.). This resonance frequency is obtained by observing the corresponding frequency for the maximum value of displacement for 0.5 V rms input voltage. Figure 4.2 shows the values of displacement versus input voltage.

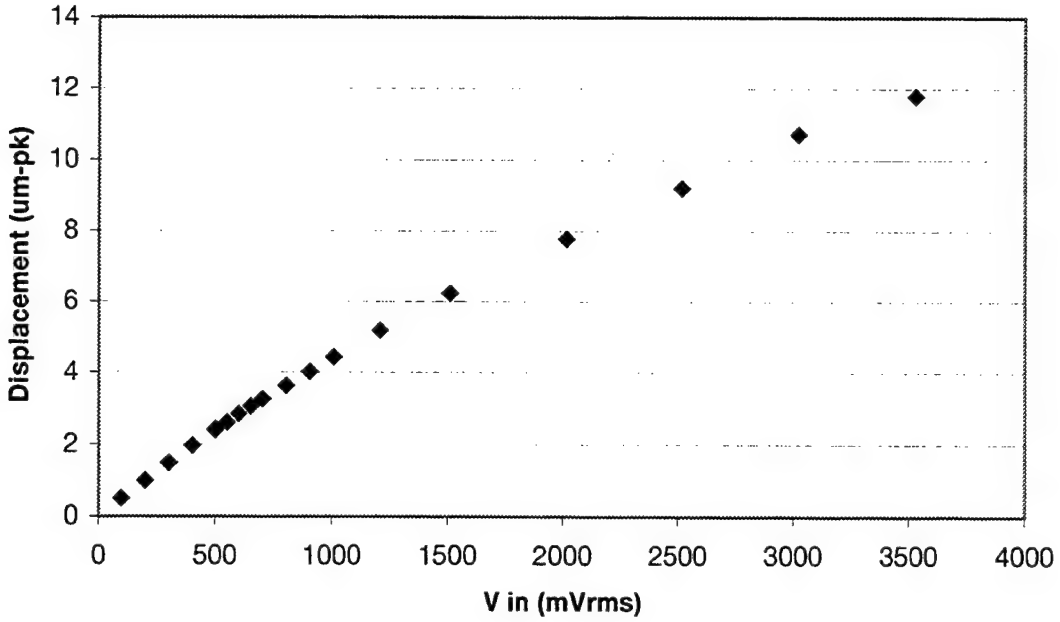

Figure 4.2. Displacement vs. Input Voltage

The laser vibrometer used for the displacement measurements has two different sensitivity scales; 4.9 mm/s·V and 24.9 mm/s·V. 4.9 mm/s·V scale is more sensitive but it can be used only for output voltages below 10 V which is the saturation limit of the instrument. 24.9 mm/s·V scale is less sensitive but good for higher input voltages. Up to 2 V input voltage, output voltage was below 10 V at 4.9 mm/s·V scale. After that the scale needed to be shifted from 4.9 mm/s·V to 24.9 mm/s·V. The distortion of the graph around 8 Volts input is a result of this shift.

The first experiment provides information about the velocity and the displacement of the piezo disk. This information is useful but not sufficient

for the design of the mini TAR, as the conditions for the piezoelectric driver in a miniTAR unit will be different than the conditions for the piezo disk used in displacement measurements.

In this experiment there was no resistance on the surface of the disk other then the atmospheric pressure and the emitted sound waves. Moreover, the effect of nearby acoustic resonances was also minimized by placing a foam rubber piece (that functioned as a sound absorber) in front of the piezoelectric disk. The effect of acoustic gas resistance in the miniTAR tube is ignored in first measurements. But, in fact, the acoustic gas resistance applied to the surface of the piezoelectric disk will significantly reduce the displacement amplitudes compared to those measured here.

In a miniTAR, the pressure (arising from the resistance of the standing wave in the tube) applied to the disk will be higher than atmospheric resistance. To simulate the effect of a strong resisting force, a small mass can be attached to the surface of the disk. Mechanically, the small mass and the gas resistance are not the same. The resistive forces for the mass are reactive, whereas those for the gas are expected to be resistive in phase. The goal was to measure the amount of force generated by the piezo disk when the resisting forces are large enough to limit the displacements greatly.

In order to be able to attach mass on the surface of the piezoelectric disk, the paper cone, which was originally attached to the disk, needed to be

removed. This removal makes a difference in the resonance frequency of the driver and the displacement amplitudes.

The resonance frequency dropped from 4120 Hz to 4070 Hz, but the displacement values increased significantly. The displacement amplitude for 15 V driving voltage was approximately 12 μm in the first transducer with the paper cone. By removing the paper cone, it was possible to get the same displacement amplitude with a 3.5 V driving voltage.

The measured displacements for the transducer without the paper cone are as follows:

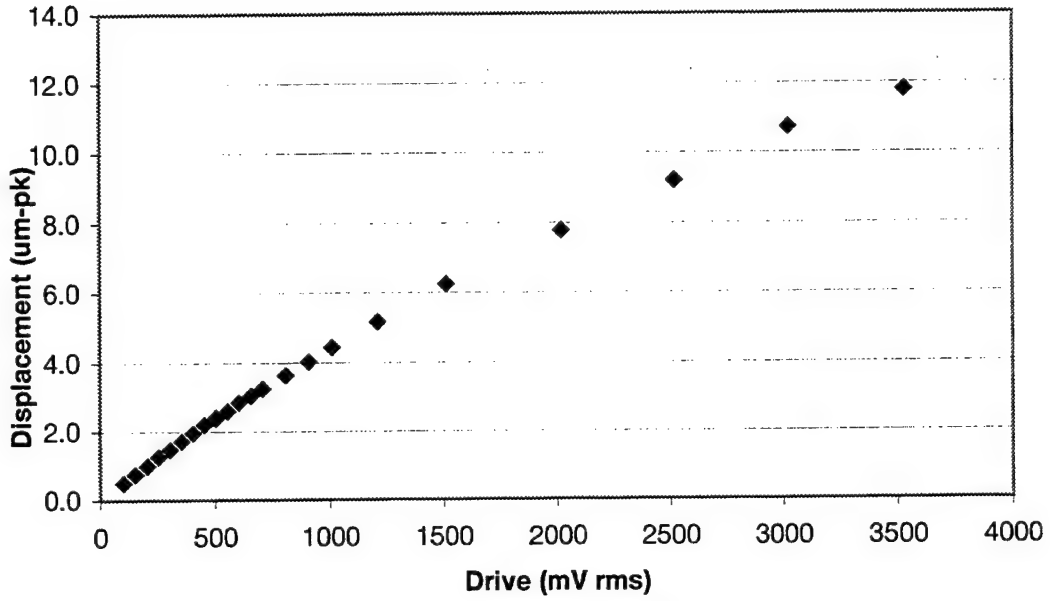

Figure 4.3. Displacement Vs. Input Voltage for a piezoelectric disk without paper cone

C. DISPLACEMENT WITH MASS

To improve the accuracy of the data, the experiment was repeated four times using different amounts of mass for each trial.

For the purpose of understanding the experimental procedures, the following explanation of how mass was attached on the disk is provided. A foundation was permanently glued on the surface of the piezoelectric disk. To increase the mount of mass, additional mass was simply screwed onto this foundation. The following figure demonstrates how this feat was accomplished.

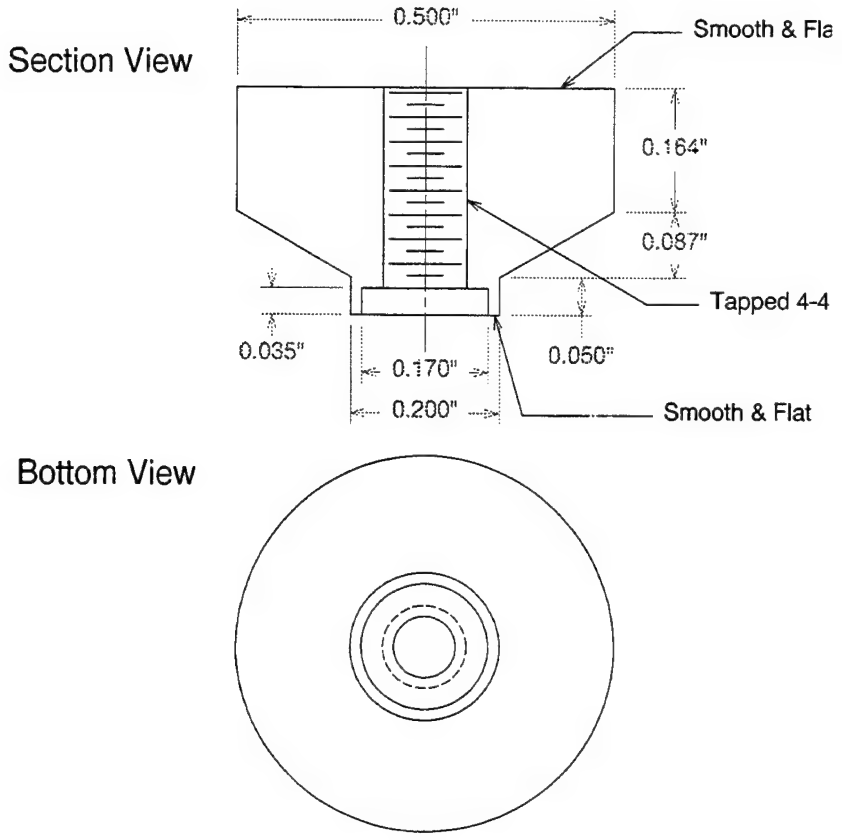

Figure 4.4.Cylindrical Mass Load

The process of displacement measurements is divided into two parts; each part is divided into four subdivisions. For the first part of the measurements, the foundation itself constitutes the mass (1.78 g.) Instead of changing the mass, the frequency is changed.

Initially, the resonance frequency of the miniTAR was 4.65 kHz. Attachment of the foundation to the surface of the piezoelectric disk dropped the resonance frequency to 3.3 kHz. Two displacement measurements were made at driving frequencies of 4.65 kHz and 3.3 kHz. To get a better understanding, displacement measurements were taken again at 4 kHz and 5

KHz. The following graph shows the displacement values versus driving voltages at different driving frequencies for the same amount of mass.

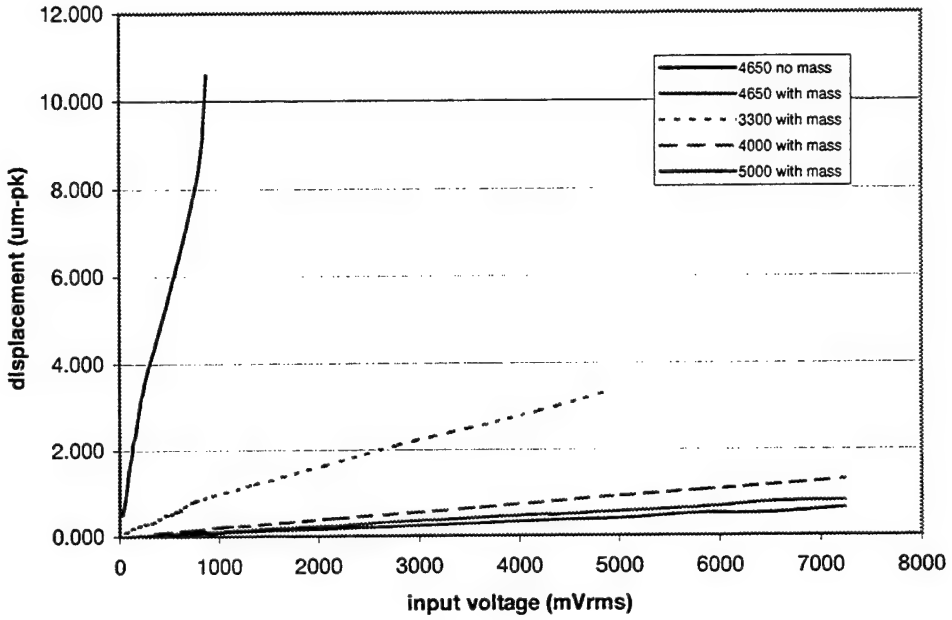

Figure 4.5. Displacement versus input voltage with constant mass at different frequencies

In the second part of the displacement measurements with mass, the frequency is kept constant at resonance frequency of 4.65 kHz. The amount of mass is increased by screwing additional mass onto the foundation. The following figure shows displacement versus input voltage for different amounts of mass. The distortion around 4 V input voltage for the measurements using only the foundation itself (m = 1.78 g) is caused by the shift of the vibrometer sensitivity scale. Displacement measurements for the same input voltage on the two scales were slightly different. The output of the higher scale was 3% below the output of the lower scale. There is no

distortion shown in the other graphs because the output voltage n exceeded 10 V rms for the applied input voltages.

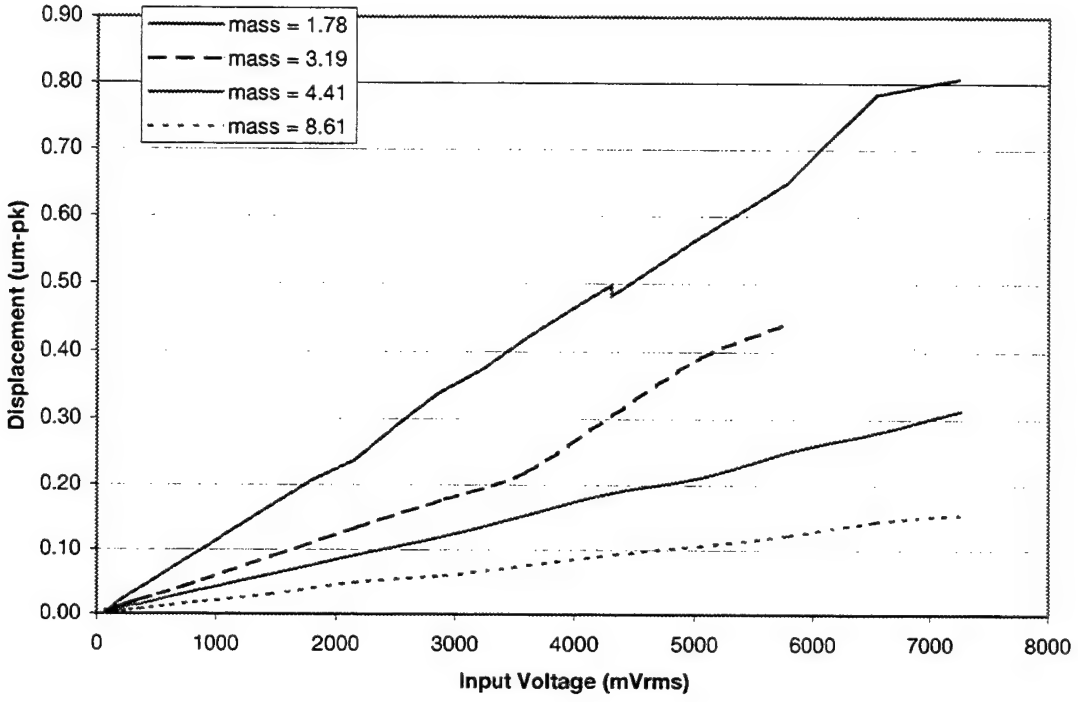

Figure 4.6. Displacement at constant frequency (f=4.65 kHz) for different mass amounts

Because of the output voltage limitation of the laser vibrometer, it was not possible to measure displacements for higher input voltages with the current setup. Therefore, for the next displacement measurements, a fiber-optic sensor is used instead of the laser vibrometer. The fiber-optic sensor is not as sensitive as the laser vibrometer and it is possible to measure higher displacements with it. Another advantage is that the fiber-optic sensor has no physical components that actually touch the disk thereby eliminating extraneous mass. With the laser vibrometer, a reflective piece of material is

attached to the surface of the disk, and even though the mass and the effect of the material is relatively small, it is not totally negligible.

Despite these advantages, measurement with a fiber-optic sensor also has disadvantages. The sensor must be very close to the moving part (piezoelectric disk). The distance between the sensor and the disk is very critical. If it is too close, the sensor may touch the disk and distort the measurements. The distance from the sensor to the disk is approximately 0.5 mm, and must be maintained throughout a given measurement. Another disadvantage is the effect of extraneous room light. If the sunlight or the light in the room is too intense, then that light will affect the measurements.

The diameter of the sensor is much smaller than the diameter of the piezoelectric disk, and the sensor is typically directed to the center of the disk. Because the value of the displacement of piezoelectric disk is greatest at the center, the need to accurately measure displacement at the center is a critical aspect of the investigation.

The displacement amplitudes were significantly lower than the amplitudes measured by laser vibrometer. The new values were one-third of the previous values. One reason for that was the rubber band on which the piezoelectric disk was placed. The rubber band created a kind of resistance and decreased the displacement.

The following is a graph of output voltage versus input voltage obtained by using the fiber-optic sensor.

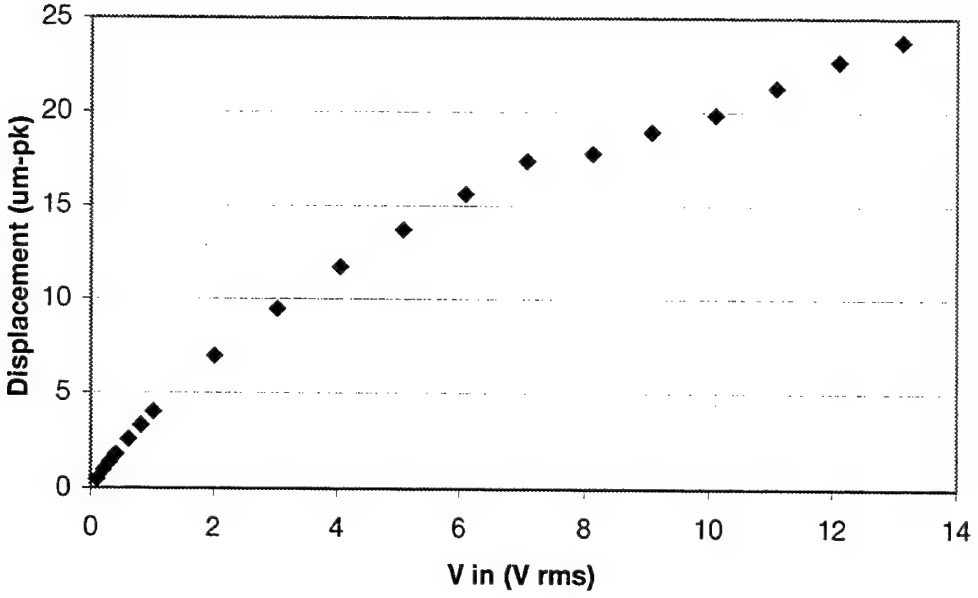

Figure 4.7. Displacement vs. input Voltage with fiber-optic sensor

V. PLASTIC MINI TAR DEVICE

A. THE DESIGN OF THE PLASTIC MINI TAR

Before designing the steel mini TAR, which will be pressurized and hermetic, a simple plastic mini TAR is created as a working model for determining the refinements which should be made on the steel mini TAR. The plastic mini TAR operates with 1 Atm of air is not hermetic. The plastic mini TAR's refrigeration performance is far below the expected performance of a steel mini TAR. However, it is much cheaper and easier to design a plastic mini TAR. It is also easier to make modifications on a plastic mini TAR rather than on the steel model.

The plastic mini TAR is intended to be simple, cheap and functional. The term "functional" refers to the plastic mini TAR's ability to cool to an acceptable level for experimental purposes. The plastic mini TAR's limited capacity to refrigerate (to 10° C only) is not an acceptable standard for a steel mini TAR. However, the plastic mini TAR is sufficient for experimental use as it is basically used as a working model rather than a permanent component.

The plastic mini TAR uses an existing Motorola (now CTS Wireless) piezo driver device instead of a specially designed driver. Since the Motorola driver has a paper cone that is capable of moving substantial volume

velocities at a low acoustic impedance, it is highly compatible with the simple plastic mini TAR's design. In this design, the driver couples to the acoustic resonator at a low acoustic impedance point in the standing wave.

The plastic mini TAR design does not deliver good refrigeration performance in general. One reason is that 1 Atm of air is not a good working medium for thermoacoustic heat engines. Another reason is that acoustically stimulated convective currents move substantial amounts of heat towards the cold end of the stack. However, it is quick and easy to build given the off-the-shelf Motorola driver.

The second part of the mini TAR is the resonator. The resonator design is similar to the original thermoacoustic refrigerator. It is a tube approximately a quarter wavelength in size and is capped at one end (near the stack). The tube opens into a dead volume near the paper driver cone. The following figure shows the design of resonator and the plastic mini TAR.

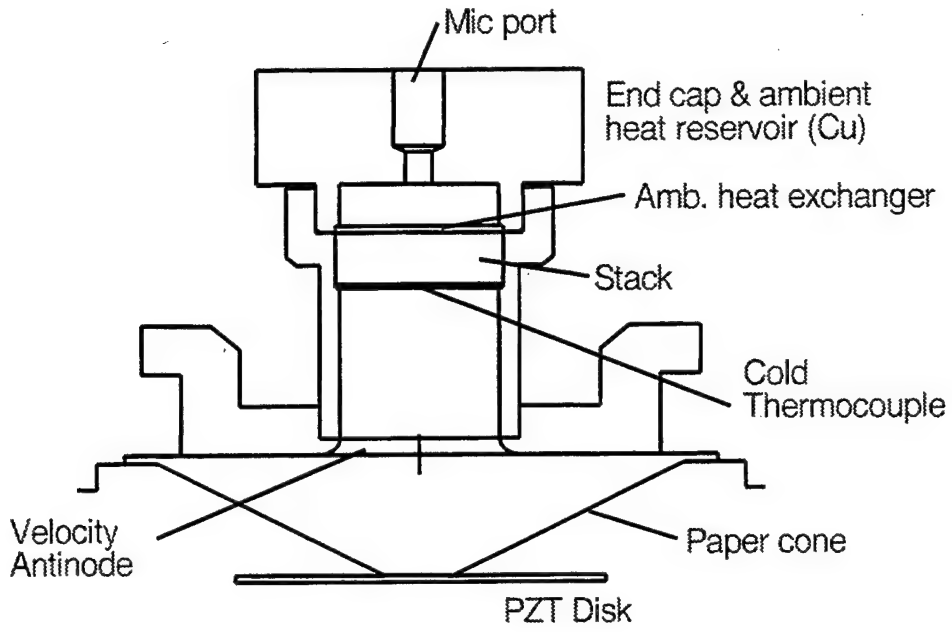

Figure 5.1. The design of the plastic mini TAR

This design was chosen because the resonator impedance matches well with the existing piezo disk and paper cone. This acoustic impedance is very low compared to the impedance at the stack.

B. MEASUREMENTS

1. Test Resonator and Coupled Resonances

Acoustic pressure amplitudes of approximately 7% to 8% of 1.014 bar (peak) at 4 kHz are measured with a simulated stack as an acoustic load-- a promisingly large value. The working medium is air at 1 Atm.

These pressure amplitudes were achieved with a drive voltage of about 15 V rms applied to the piezo disk, through a 4 ohm resistor (to protect the power amplifier from instabilities with a capacitive load.). Some piezo disk damage and loss of drive sensitivity was experienced at drive voltages in the neighborhood of 20 V rms. Further discussion regarding this damage and loss can be found in Chapter IV.

Determination of the precise resonance frequency, prior to building the resonator shown in Fig. 5.1, is necessary to obtain the maximum acoustic pressure amplitude. The concern is the optimum length of the tube, as this will affect the resonant frequency of the tube. The difficulty is that both the piezo disk and the acoustic resonator are independently resonant, and that for best power and efficiency, the two resonance frequencies should be approximately equal. Also, the resonance frequency of the piezo disk changes slightly with the magnitude of the input voltage. Theoretically, approximately a quarter wavelength for the tube length gives the highest amplitudes. The resonance frequency of one piezo disk was 4090 Hz. From the following equations, the wavelength and the quarter wavelength can be obtained:

$$\lambda = \frac{c}{f} = \frac{344\ m/s}{4090\ Hz.} = 0.0841\ m = 84.1\ mm \tag{5.1}$$

$$\frac{\lambda}{4} = \frac{0.0841}{4} \approx 0.021\ m = 21\ mm \tag{5.2}$$

Since the acoustic impedance of the driver and tube must be matched for optimum performance, this will cause the resonant frequency of the combined system to slightly different than either of the two independent resonances.

Because of this uncertainty, a simple resonator test apparatus was built prior to the device shown in Fig. 5.1. The test resonator, shown in Fig. 5.2, has a pressure transducer mounted in a sliding end-plug. The plug is sealed in the quarter wave tube with a "piston" type O-ring seal seen as a black ring at the bottom of the aluminum plug in the figure. A small wad of clean stainless steel wool was inserted into the resonator near the end plug to simulate the added dissipation of a thermoacoustic stack.

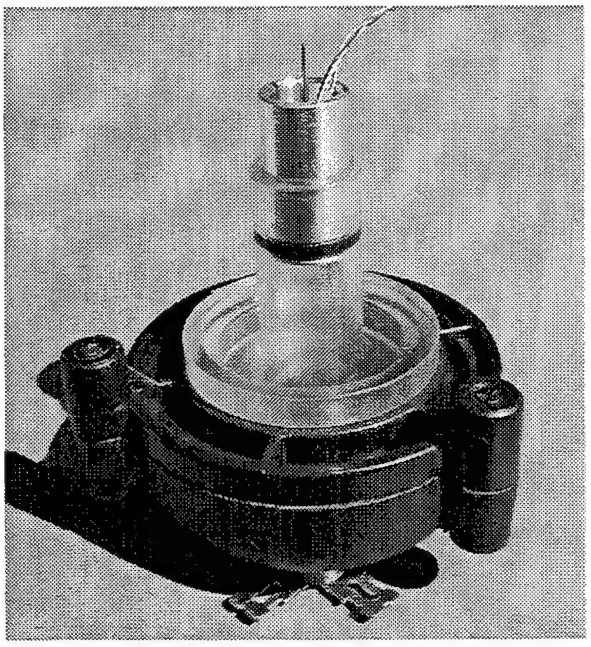

Figure 5.2. The test resonator and piezo driver, 5.8 cm in total length.

The first measurements were swept sine transfer functions of pres response relative to the drive voltage, performed at low amplitudes. Seve of these were measured while varying the resonator length. The highe peak in the pressure transfer function was obtained with a tube length o 20.4 mm at a frequency of 4.075 kHz. This result is within a percent of the simple result of Eq. 5.2. A plot of this particular transfer function is shown in Fig. 5.3.

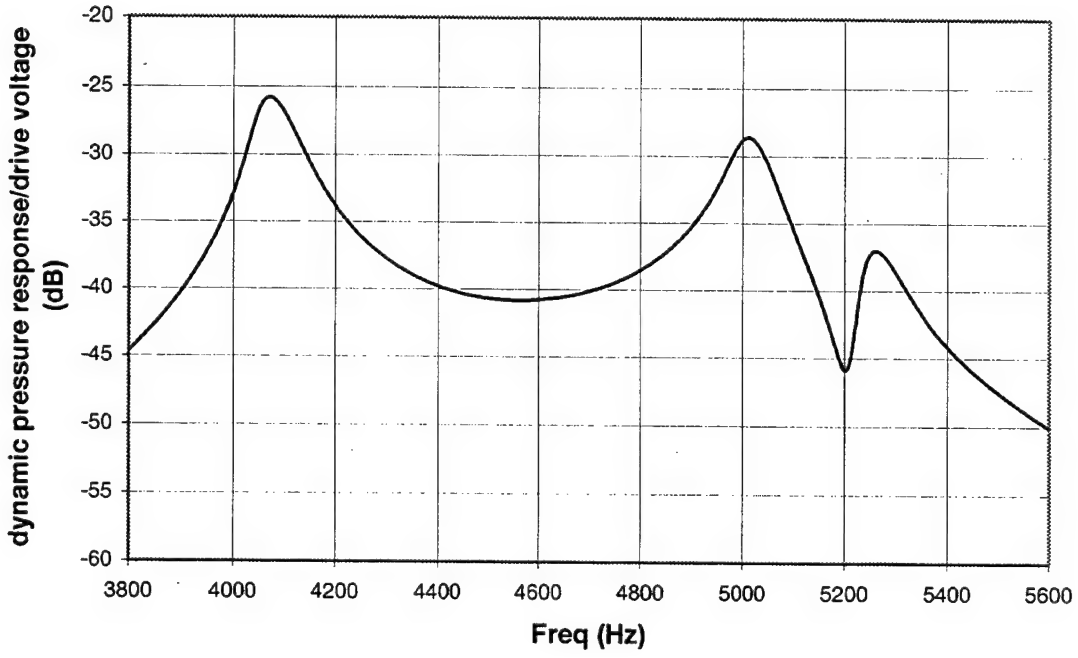

Figure 5.3. Test resonator dynamic pressure response curve. Pressure sensor sensitivity is 280.0 mV/psi.

Note that a second peak shows up at 5 kHz. This peak is consistently 3 dB less than the one near 4 kHz when the resonator length is varied. While this vibrational mode the piezo disk could be used in a mini TAR, the cooling

performance would be considerably less. The maximum cooling power at 5 kHz would be approximately half that obtained at 4 kHz.

The second group of test resonator measurements determined the pressure response linearity and maximum amplitude. For this experiment, the input voltage started at 0.25 V rms, increased to 15 V rms and then decreased to 0.25 V. The microphone voltage is basically measured twice for each input voltage to observe any possible changes. This procedure should ensure that piezoelectric damage at the highest voltages would be detected. The first measurement is taken during the voltage increment phase, and the second during the voltage decrement phase. Also, the drive frequency was adjusted for maximum pressure response for each data point. The measurements show that the output voltages have less than a 3% difference, which is probably not significant.

The following graph shows the measured voltages with the microphone placed in the tube. The dashed line shows the measurements during the increment, and the solid line shows the measurements during the decrement.

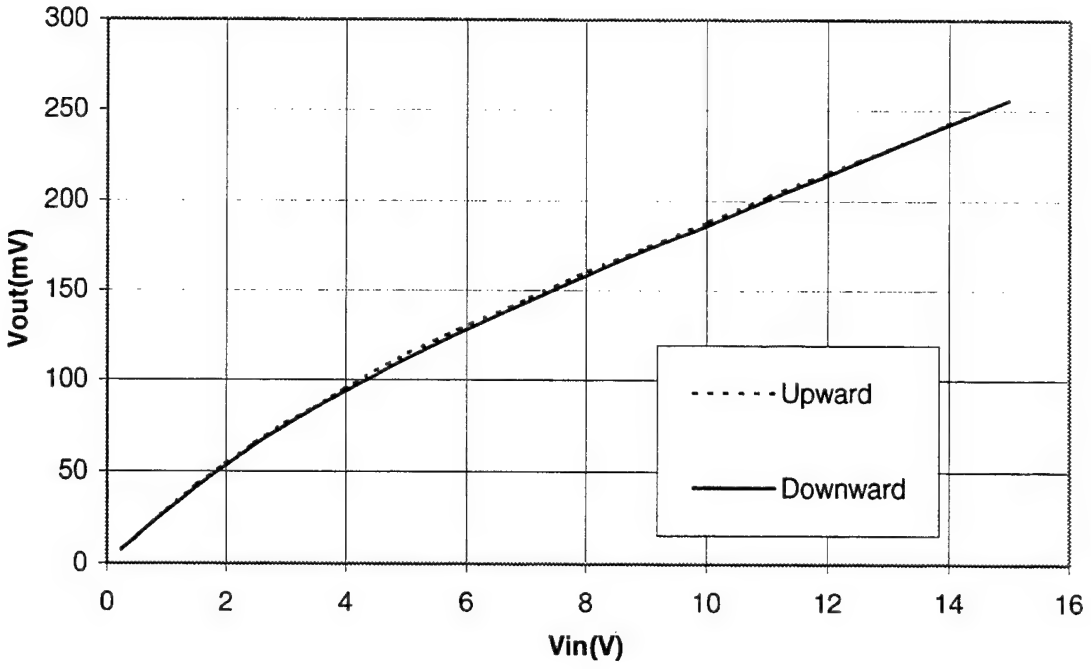

Figure 5.4. Input voltage vs. output voltage at the microphone

It was also observed that the resonant frequency of the driver and tube system decreased by roughly 4% at the highest amplitudes compared to the lower amplitudes. For this reason, the measurements were repeated at a few more tube lengths of the test resonator.

To see the effect the length of the tube on the pressure amplitudes, the length of the tube is increased from 20.4 mm to 21.9 mm. The same measurements are repeated for the new length. For low input voltages, (up to 6 Vrms) the pressure amplitudes are very close. However, after 6 Vrms, the output voltages for the setup with the 21.9 mm tube length show a 5% improvement over the initial setup. The following graph compares the output

voltages for the two different tube lengths. This longer resonator operating at a resonant frequency of 3.85 kHz was selected as the best performer, so that the plastic mini TAR design was modified for this new operating frequency.

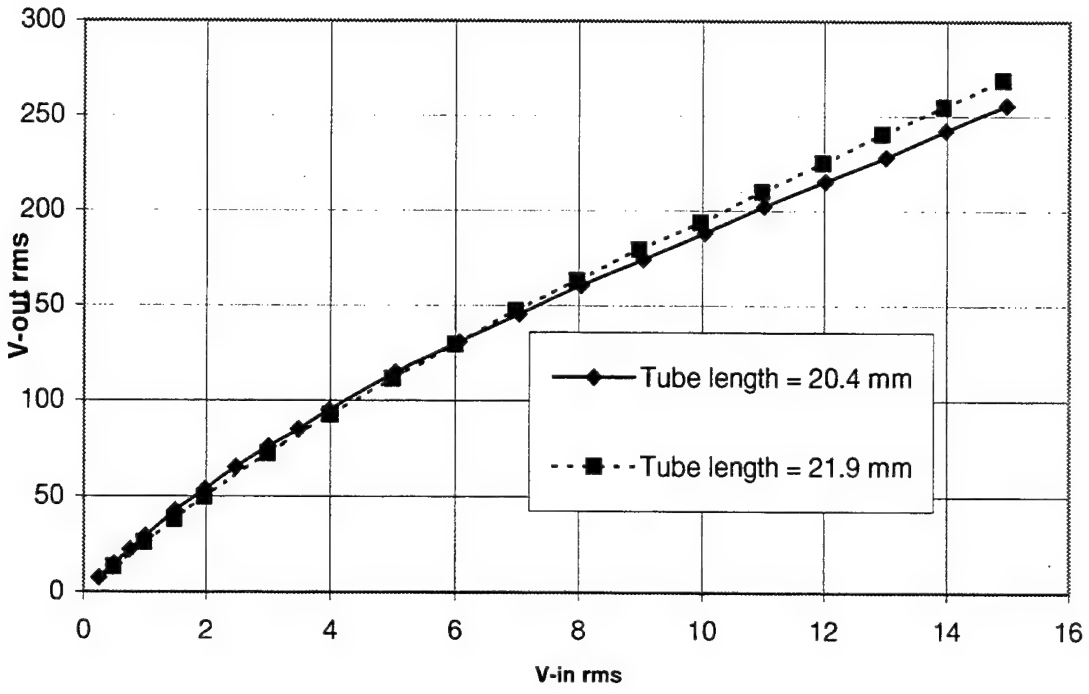

Figure 5.5. Comparison of outputs for different tube lengths

2. Refrigeration Measurements

Once the plastic mini TAR was built, refrigeration measurements were taken. The temperature difference between the cold heat exchanger and the hot heat exchanger gives the value of the refrigeration. Initially, both heat exchangers have temperature values close to room temperature and to each other. After running the mini TAR, the temperature at the cold heat exchanger decreases while the temperature at the hot heat exchanger increases. After a while, the cooling stops and the temperature at the cold heat exchanger also begins to increase. The "hot" heat exchanger has significant heat capacity, but its temperature increases with time because there is little heat rejection to the environment. Such a heat rejection path was not provided since it was not believed necessary for this proof-of-concept experiment.

Overheating at the hot heat exchanger is one contributing factor resulting in the modest cooling observed. Cooling the copper part connected to the hot heat exchanger is the recommended solution for this problem. In the experiment, the copper part is cooled every two or three minutes. The refrigeration performance of the mini TAR versus input voltage can be seen in the following graph.

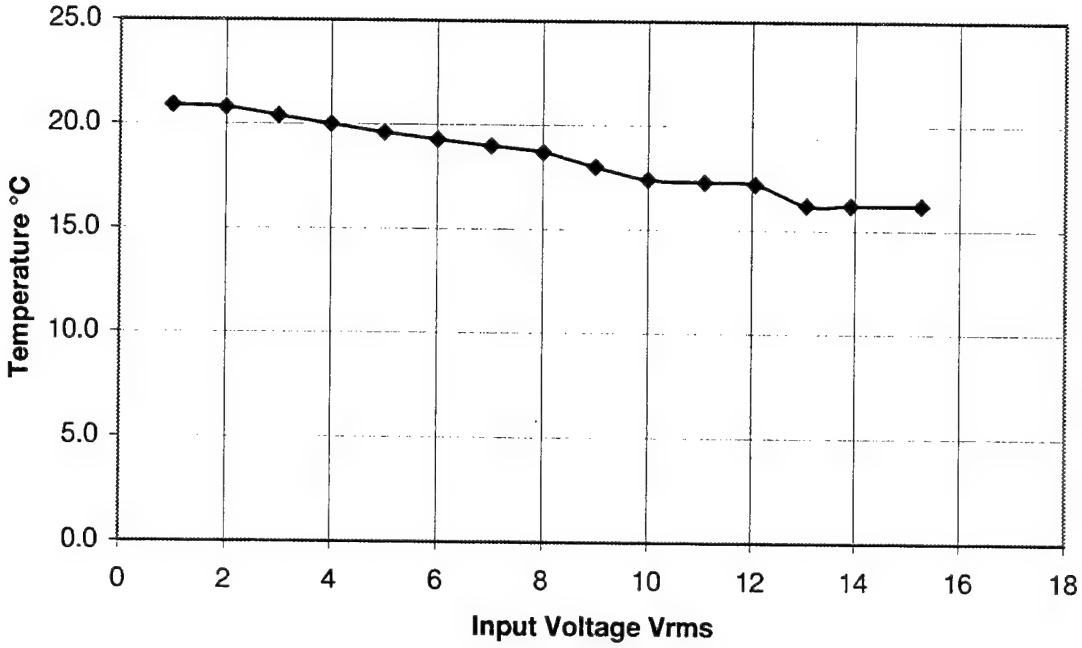

Figure 5.6. Temperature at the cold heat exchanger vs. input voltage (rms)

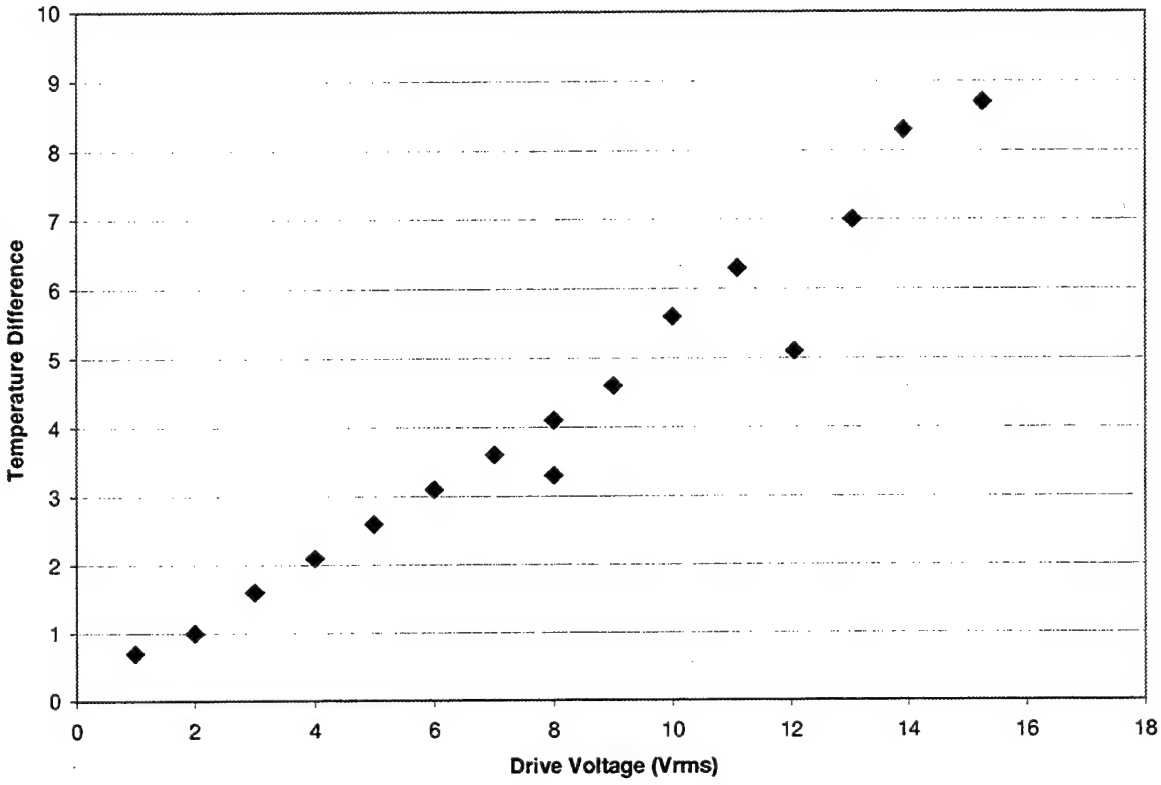

Figure 5.7. Temperature difference between the heat exchangers

A much larger temperature span was observed during a rapid cool-down experiment at a maximum drive voltage of 15 Vrms. In this measurement, a cold temperature of 14° C was observed with a "hot" heat exchanger temperature of 26° C.

During these experiments, the temperature of the piezo disk does not stay constant. The piezo disk gets hotter as a result of the energy dissipated

while being driven. The degree to which the disk heats up depends on t
input voltage and driving frequency.

The heating effect was discovered while trying to understand the drop in resonant frequency observed at higher drive amplitudes Figure 5.5 shows the temperature change vs. input voltage under conditions of no vibrational loading. While this heating effect is rather large, the effect will likely be smaller in a pressurized TAR. The thermal conductivity of helium or a helium component gas mixture is roughly a factor of 5 higher than for air.

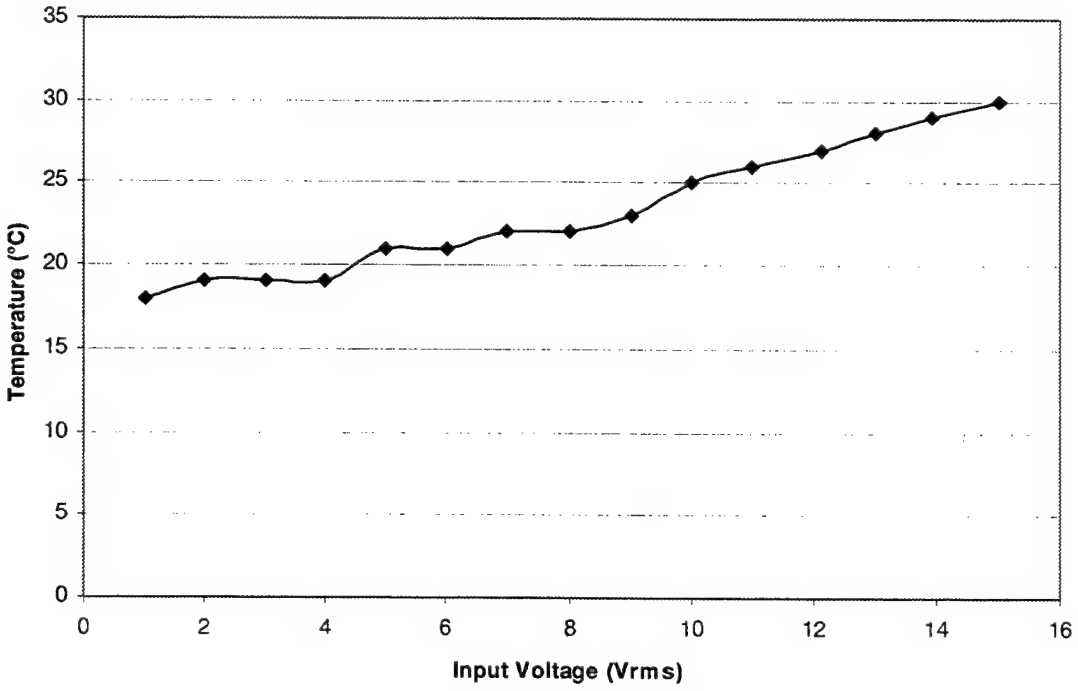

Figure 5.8. Temperature change at piezo disk vs input voltage

The cause of the frequency drop observed with the test resonator and the plastic TAR is not known. It may arise from acoustic nonlinearities, the heating effect discussed here, or most likely it is an intrinsic property of the piezoelectric material near its maximum drive voltages.

THIS PAGE INTENTIONALLY LEFT BLANK

VI. DESIGN OF MINI TAR DRIVER UNIT WITH MOTOROLA PIEZO DISK

This chapter concentrates on the design parameters of the mini TAR. These parameters are defined with computer assistance and experience. Information about how parameters are defined and the software used for simulation will be given in the following sections.

A. GENERAL DESIGN THEORY

Design is the thought process comprising the creation of a physical, temporal or conceptual entity. This process includes:

- Identification of a set of needs;
- Initial conceptualization of a way to meet those needs;
- Further development of that initial concept;
- Engineering and analysis required to make sure it works;
- Prototyping of its preliminary form; and,
- Construction of its final form.

Each of these steps contributes to the generation of form, and is thus part of the design process.

The design process is also systematic. Prototype designing of an engineering project is the first step in manufacturing a product. The

prototype design can either be done physically in real life or virtually in a computer environment. The usage of computer aided simulation programs enables designers to make modifications on their virtual designs in a short period of time and without any extra cost.

The same theory is also true for the design of the mini TAR. Before the actual design of the mini TAR, a virtual model is designed in a virtual environment. The computer makes it possible to make modifications on the project variables and observe the results. In this manner, it is possible to get the optimum design parameters, such as the dimensions or the shape of the tube, or the mini TAR's driving frequency.

B. DESIGN SIMULATION

A software program called Design Simulation for Thermoacoustic Research (DSTAR) is used for the design of the mini TAR. DSTAR is a Windows™-compliant graphical based program that provides a flexible and powerful tool for the design and analysis of thermoacoustic heat engines. The code allows the analysis of the thermoacoustic-wave and energy-transfer equations from the beginning to the end of a thermoacoustic heat engine, on a component-by-component basis. This approach allows the user to change the configuration and parameters of the individual components of the heat

engine "on the fly" with DSTAR recalculating the effect of the changes on the overall solution of the heat engine. (Curtis, 2000)

For the mini TAR, some of the parameters were defined or calculated at the inception of the project. For example, the resonance frequency of the piezo disk driver is calculated around 4.4 kHz. Initially, we intended to use a piezo disk driver operating at 10 kHz. (10 kHz is also one of the initial requirements set by Rockwell.) However, instead of building a new driver at 10 kHz, we decided to use an already existing Motorola tweeter (driver) whose operating frequency was around 4.4 kHz. Rockwell may design future mini TARs operating at 10 kHz, but the prototype explained in this thesis will operate below 5 kHz.

The parameters related to the gas in the tube were also predefined. We decided to use He-Kr gas mixture under 15-bar pressure because it should maximize the efficiency of the mini TAR and because this gas was already available in our laboratory.

Some parameters such acoustic amplitude and gas pressure can be varied at-will in the experimental phase of the project, since the refrigerator's performance does not depend strongly on these. Although, several small improvements in efficiency can be obtained by the combined adjustment of these low-sensitivity parameters.

Other parameters, or combinations of parameters, are quite sensitive to variations or errors, and must be determined precisely. One such combination is the resonator length and the drive frequency. The length of the tube components and overall tube length, were some of the parameters determined by DSTAR. The overall resonator length is considerably less than a quarter of a wavelength because of the shaped diameter changes of the resonator. The shaped tubing reduces acoustic dissipation greatly and improves efficiency, while making the resonator more compact. For 4 kHz, a quarter wavelength is:

$$\frac{\lambda}{4} = \frac{c}{4 * f} = \frac{300\ m/s}{4 * 4000\ Hz} = 18.75\ mm$$

The piezoelectric flexural disk has a its own resonance, with a rather narrow operating frequency range. Changes in the resonant frequency of the disk demand that the length of the resonator be changed correspondingly. These facts necessitate understanding and testing the operation of the disk and driver prior to completing the resonator design. Changing the resonator design to match shifts in the operating frequency of the driver can be accomplished easily with the aid of DSTAR.

C. DESIGN OF THE MINI TAR

The following section will discuss the physical parameters and the overall design of the mini TAR.

The mini TAR consists of two main parts. The first one is the driver and second one is the resonator vessel. Since the main interest of this thesis is the driver, we will focus our discussion on this topic. The following figure shows the general design of the mini TAR driver unit.

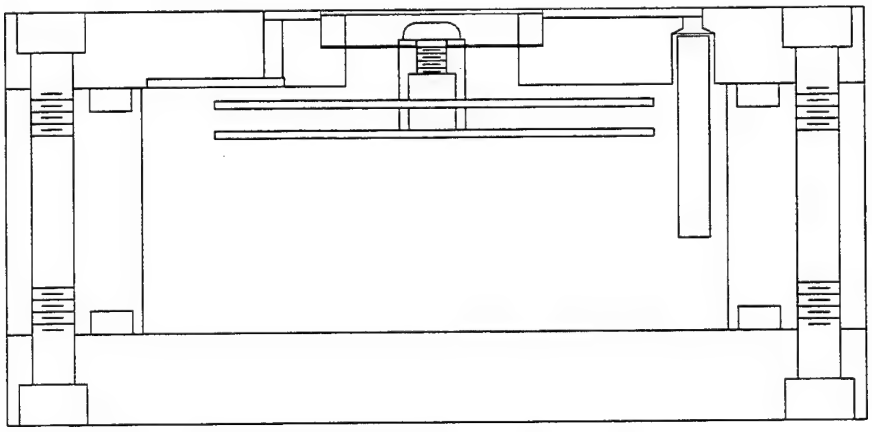

Figure 6.1. The mini TAR driver unit

The driver part of the mini TAR has also two main parts: The piezoelectric driver unit and the sealed pressure vessel unit; the latter houses the piezoelectric disk, flexible steel diaphragm, and microphone.

The piezoelectric disks are obtained from the manufacturer of Motorola tweeters. A steel diaphragm is attached to the surface of the piezoelectric disk to provide the correct impedance matching between the mechanics of the disk and the acoustics of the resonator. (The details of this assembly are explained in Chapter VII.)

The second part of the driver is composed of three parts: the top plate, the bottom plate and the body. Although it would be possible to reduce the number of subparts and/or the cost of manufacturing the subparts, it would increase the difficulty of the research project.

The main purpose of the driver is to produce the acoustic power required for cooling. The piezo disk produces vibration power. Converting this power into a useful acoustic form and delivering it to the resonator tube requires extra work.

In the mini TAR, a steel diaphragm is used to transfer acoustic power inside the tube. The dimensions and the flexibility of the steel diaphragm are very essential for the maximum generation of acoustic power. If the diaphragm is too flexible, acoustic power will be lost. The high impedance acoustic pressures being generated in the resonator will force portions of the

soft diaphragm to move in directions opposite to each other. A representation of this undesired effect is shown in the following figure.

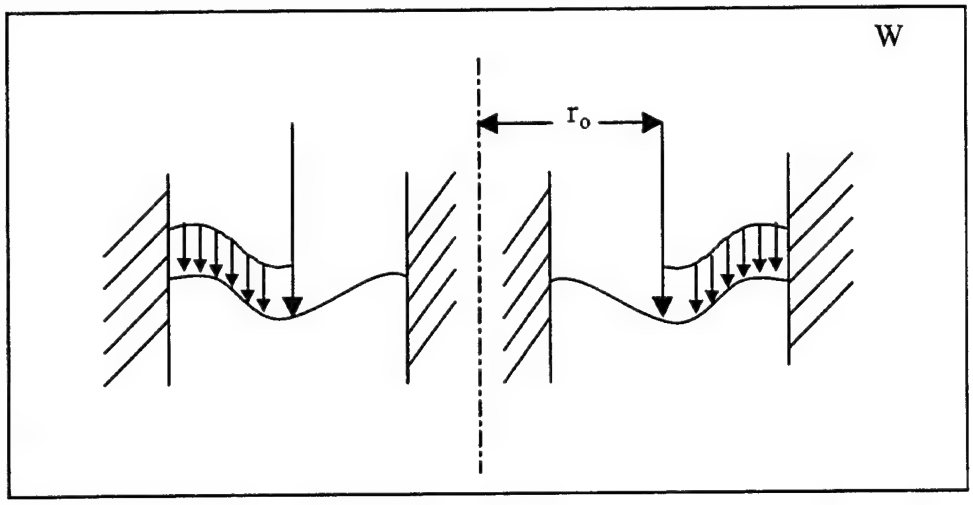

Figure 6.2. The motion of the soft steel diaphragm

As a result, the magnitude of the volume displacement will be relatively small. Another disadvantage of having a soft diaphragm is that the diaphragm may suffer damage after a certain period of operation.

On the other hand, a steel diaphragm that is too firm has disadvantages as well. The force of the piezo disk may not be enough to produce enough displacement.

If the stiffness and the flexibility of the steel diaphragm have the right values, the displacement of the diaphragm will be as follows:

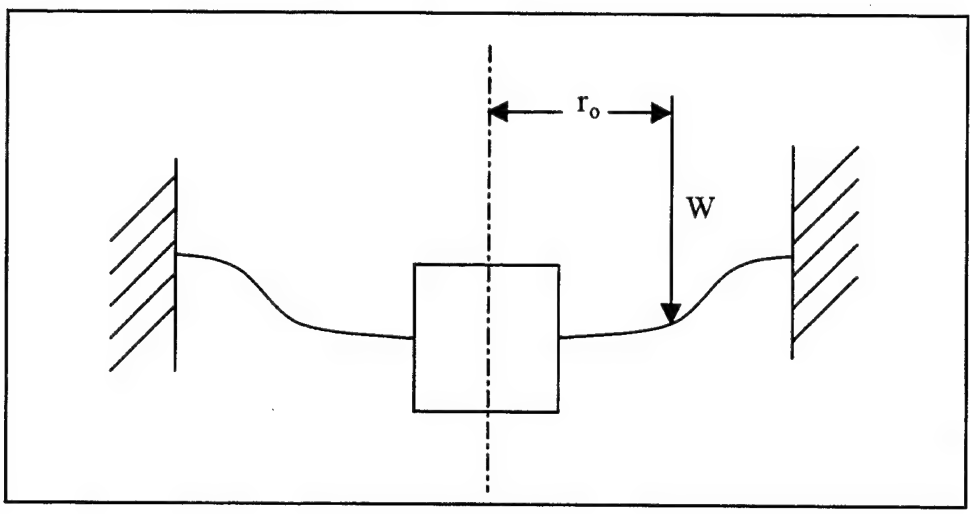

Figure 6.3. The ideal motion of the steel diaphragm

VII. ASSEMBLY

As mentioned in the previous chapter, the mini TAR driver is composed of three main parts: the top plate, the bottom plate and the driver body. Each part includes smaller components. This chapter describes in detail the assembly of the main parts as well their smaller components. Information about the mini TAR's assembly is provided for a better overall understanding of the mini TAR and to highlight potential improvements.

A. ASSEMBLY OF THE TOP PLATE

Since the top plate is comprised of both the piezo disk and the steel diaphragm, it is logical to assert that this component is the most critical. The basic function of the mini TAR driver, which is to deliver acoustic power to the resonator, happens here.

The amount and the amplitude of the acoustic pressure produced by the driver depend on the parameters of the driver. The frequency and the amplitude of the driver are two such parameters, but these can be configured during the mini TAR's operation.

On the contrary, parameters such as the diameter and the shape of the steel diaphragm are not alterable once they have been established. The values of these elements are predefined by calculations and prior developmental work to give the optimum results for high performance.

During assembly, any small manufacturing flaw can change the values and affect the overall performance of the mini TAR. (Detailed information about potential errors will be provided later in this chapter.).

The top plate is one of the three main parts of the mini TAR driver, and consists of smaller parts including the capillary tube, steel diaphragm, and piezo disk. The following figure shows the design of the top plate from top to bottom.

Mini Driver Top
Make 5 of 6061-T6 Aluminum
Notes: X.XXX tolerance is ± 0.003"; X.X° tolerance is ± 0.05°.

Tom Hofler
Physics
Room SP-142
X-2420
tjhofler@nps.navy.mil

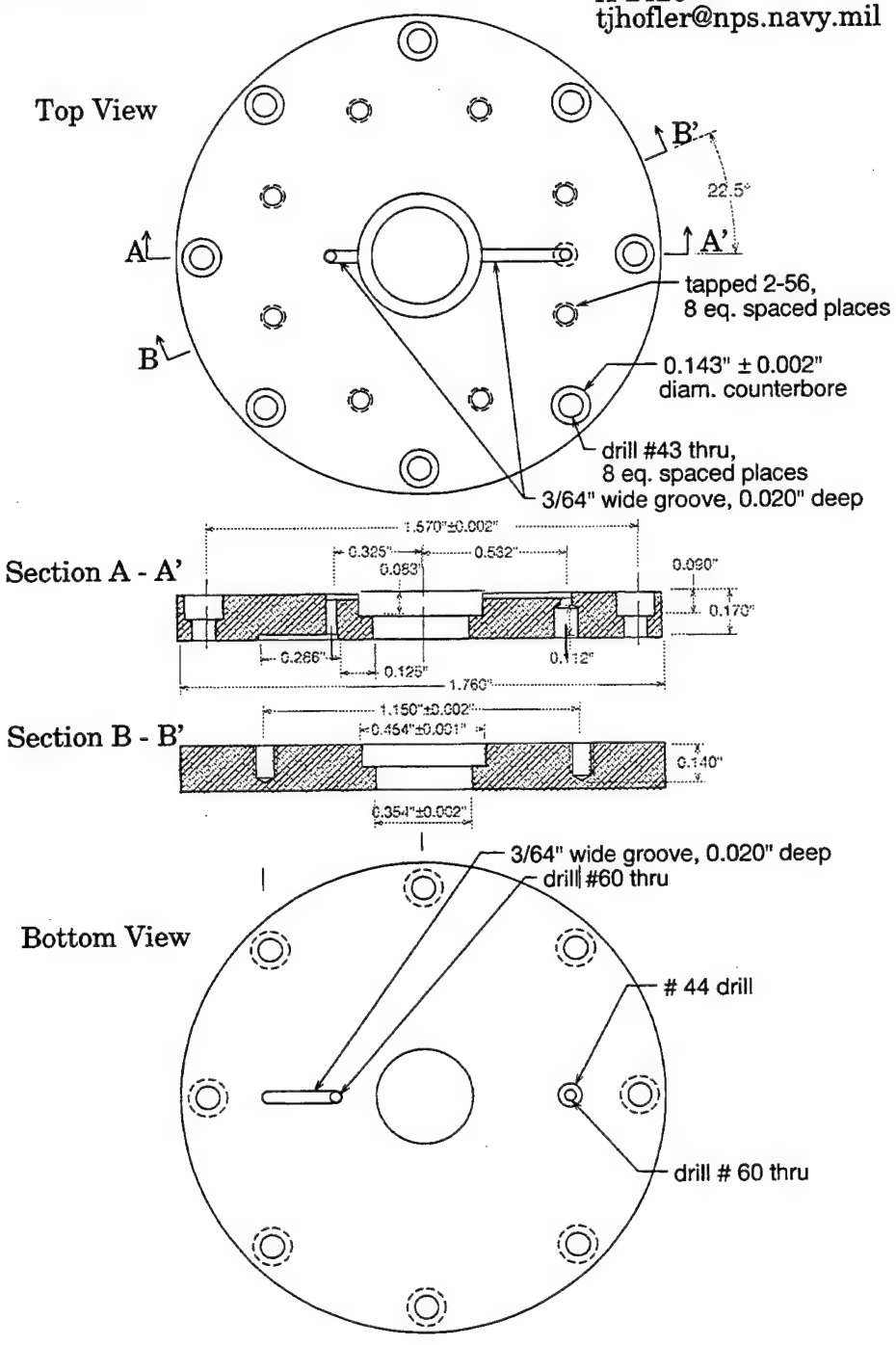

Figure 7.1. The design of the top plate

One of the most important parts of the top plate is the capillary tube. The capillary tube is required for static pressure equalization and passes through the top plate as shown in Figure 6.2. Additional information about the function of the capillary tube can be found in Chapter VII. In this chapter we will concentrate on the assembly of the capillary tube.

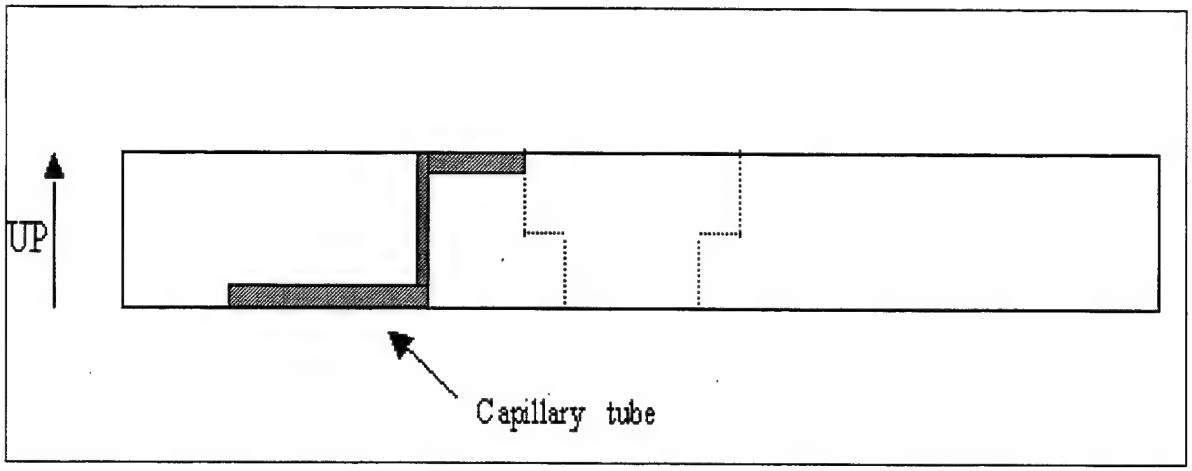

Figure 7.2. The capillary tube used for pressure equalization

The diameter of the capillary tube is very crucial and must be precise. If the diameter is too small, then there will little gas transfer. If the diameter is too big, it will reduce the dynamic acoustic pressure.

Special care must be taken to avoid blocking the capillary tube while gluing it to the top plate. (We used one-hour epoxy for gluing.) If the capillary tube is blocked, there will be no pressure equalization. A lack of pressure equalization will prevent purging and filling of the resonator with the

intended gas. Furthermore, partial blockage of the capillary could cause damage of the steel diaphragm, since it can only sustain a pressure difference that is small fraction of the intended static pressure of the resonator. The cutting and the bending of the capillary tube must also be done cautiously; a small mistake could also block the tube.

B. ASSEMBLY OF THE BOTTOM PLATE

Assembly of the bottom part is similar to that of the top part except there is no steel diaphragm or piezo disk.

There are four holes on the surface of the bottom plate. Three of them are for the power supply and microphone cables. The remaining hole is for injecting gas inside the mini TAR and increasing the pressure.

The installation of the power supply cables is relatively easier than the installation of other cables. Instead of allowing cables to pass through the holes, two mini banana jacks are installed on the back plate.

The mini banana jacks are gold plated with solder terminals on the backside. A small gauge wire is soldered onto each before epoxying. The exterior of the jacks are roughened with medium grit sand paper. Only a small amount of epoxy is left under the front lip of the jack to separate it from the aluminum plate. This epoxy is filled with tiny glass particles and will eliminate the conductivity between the plate and the jack.

After installation, but while the epoxy is still fluid, the electrical continuity is checked with gentle pressure. The electrical resistance is found to be between the range 100 K ohms and 1 M ohm. Although this resistance means there is conduction, this amount of conduction is typical of ionic transport in the wet epoxy and usually disappears when the epoxy is fully cured.

Black epoxy is used to glue the mini banana jacks to the bottom plate. Since it has small glass particles in it, black epoxy is very good for eliminating conductivity. The other function of the black epoxy (and one hour epoxy used for gluing other parts) is to prevent gas leakage.

Epoxy makes a good gas seal, although a small amount of helium diffusion will occur in any organic material, with metals being the only perfect sealing substance. This small amount of leakage can be minimized further by ensuring that the diffusion path inside the epoxy is as long and narrow as possible. By decreasing the number of holes, it is possible to decrease the usage of epoxy and the magnitude of the leakage. The microphone and the hole for the microphone are just for scientific measurements and are not operating parts of the mini TAR. Thus, they can be eliminated for large scale production. And for the power supply, theoretically one hole and one cable passing through it could be enough. We can supply positive current thru this one cable and use the body of the mini

TAR for grounding. But this will bring some other issues like the isolation of the mini TAR which could cause problems for scientific measurements.

The installation of the microphone is relatively more complex than the installation of the power supply cables. All of the four bare copper microphone wires must pass through one small hole. Using insulated wires may not be appropriate, because the pressure inside the mini TAR may pass through the space between the wire and the insulation material. The only way to prevent leakage is to remove the insulation material from the wires and to use bare wires.

The usage of black epoxy will prevent the leakages in the hole, although there is no way to put black epoxy inside the cable. The black epoxy will separate the cables from each other as well as from the bottom plate of the mini TAR.

The third and the last main part of the mini TAR driver is the side part, which is the sidewall of the cylinder shaped driver. Since there are no subparts on the surface of the side part, no further information is given about its assembly.

The following section explains how main parts are attached to each other.

C. THE INSTALLATION OF THE MAIN PARTS

The last phase of the assembly is the attachment of the three main parts to each other. There are holes for screws on the surfaces of all parts. The screws may be enough to hold the parts together; however, they are not enough to prevent gas leakage. Additional components are needed to eliminate or reduce the gas leakages. For example, rubber O-rings are required between the parts to make the whole structure leak-proof. The driver top plate is sealed to the resonator flange with a thin Teflon gasket, to prevent helium gas leakage.

VIII. TESTS

Tests are an integral part of development during all of the steps of the life cycle of a project-- there are even tests during the mass production and operating phases. However, the focus of this thesis is on pre-production tests. Chapter 4 discusses the displacement measurement tests of piezo disks, and Chapter 5 details the performance tests of the plastic mini TAR. Finally, this chapter tests the volume displacement and the overall performance of the prototype mini TAR driver.

A. VOLUME DISPLACEMENT

One of the two measurements in this chapter is the volume displacement measurement. As in the displacement measurements explained in Chapter 4, a laser vibrometer can be used. However, due to the range limitations of laser vibrometer, it is impossible to make measurements at high drive voltages where the vibration response exceeds the range of the instrument.

Another approach is to use a microphone to measure the acoustic pressure produced by the driver. However, there are some limitations on its effectiveness.

Since the measurement was performed in a room with ambient noise, the sound level produced by the driver must be much higher than the noise

level. Initially the microphone was placed within 3 mm of the driver diaphragm. The measured sound pressure levels in this configuration exceeded the maximum range of our sound level meter, at 130 dB SPL. The microphone was subsequently placed 3 or 4 cm from the diaphragm. In this configuration, sound pressure level measurements were within range at the highest drive levels and the signal to noise ratio was still good at the lowest drive levels.

While it was assumed that the measured sound pressure level was proportional to the motion of the driver diaphragm, the constant of proportionality was not known.

One way to capitalize on the strengths and minimize the weaknesses of the two approaches is to use both simultaneously and combine the resulting data. Since the units of measurement are not the same, combining the data will indicate a comparison of the linearities or nonlinearities of the measurements. If the linearities of the measurements are the same, we can predict the response and the displacement of the mini TAR at higher driving voltages.

The first part of this comparison is the displacement measurements with laser vibrometer. The following graph shows the measured displacement values at applied driving voltages.

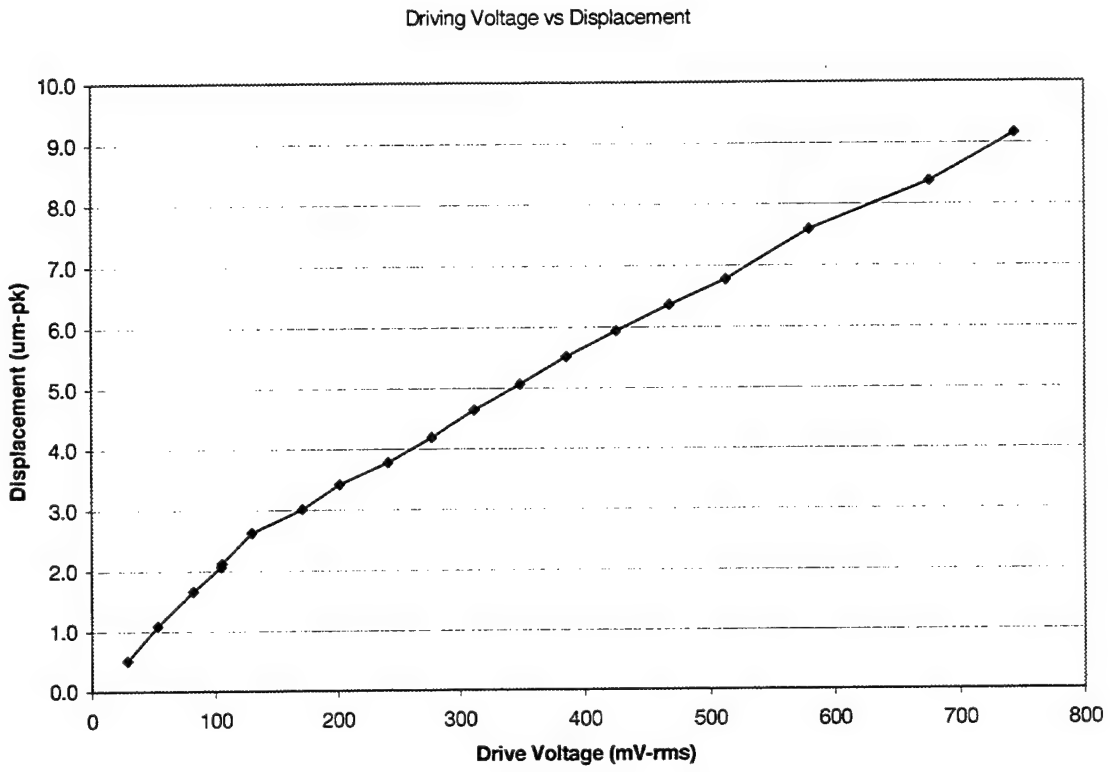

Figure 8.1. Displacement measurements

The second part of the comparison is the sound pressure level (SPL) measurements of the mini TAR driver. The signal from the microphone was measured with a digital oscilloscope. Since the main purpose of this measurement is to check the linearity of the driver response, the output voltages on the oscilloscope were not converted to an absolute sound pressure scale.

The following graph shows the output response of the mini TAR c
in terms of microphone signal versus driving voltage.

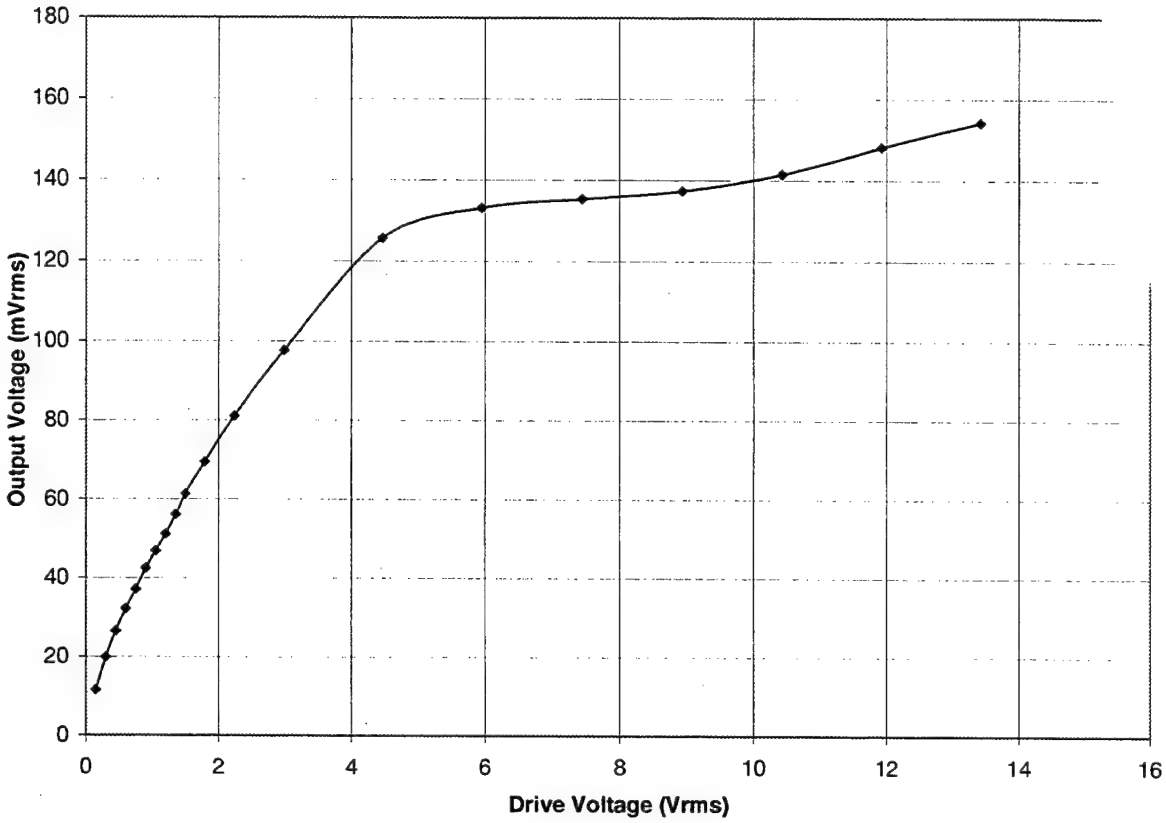

Figure 8.2. Sound pressure response measurements of the mini TAR driver

As seen in the graph, the measurements are quite linear up to 5 Vrms. After 5 Vrms, the graph becomes nonlinear. Since the first part of this graph (up to 5 Vrms) is the main area of interest, the results are still applicable for the purposes of our initial comparison.

The frequency response of the driver gives us information about the general response of the driver. For frequency response measurements we keep the voltage constant and sweep the frequency between the previously defined limits.[1] For better observation we repeated each measurement (with microphone) twice first sweeping up and second sweeping down.

This experiment is repeated for several different driving voltages. Here we are going to present only two of them.

The following graph demonstrates the frequency response for 146 mV driving voltage.

---

1 Lower limit 4 kHz and upper limit 5 kHz.

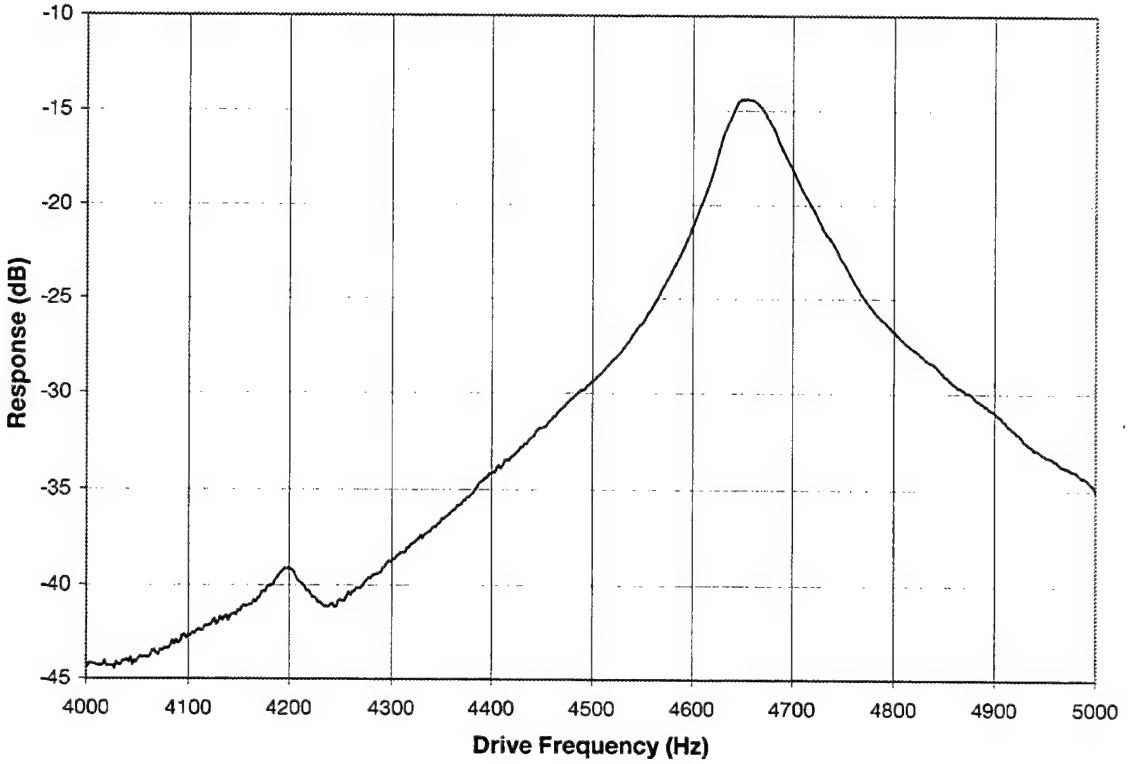

Figure 8.3. Frequency response of the driver at 146 mVrms driving voltage (Microphone measurements)

The following shows the frequency response as well however at a much higher driving voltage.

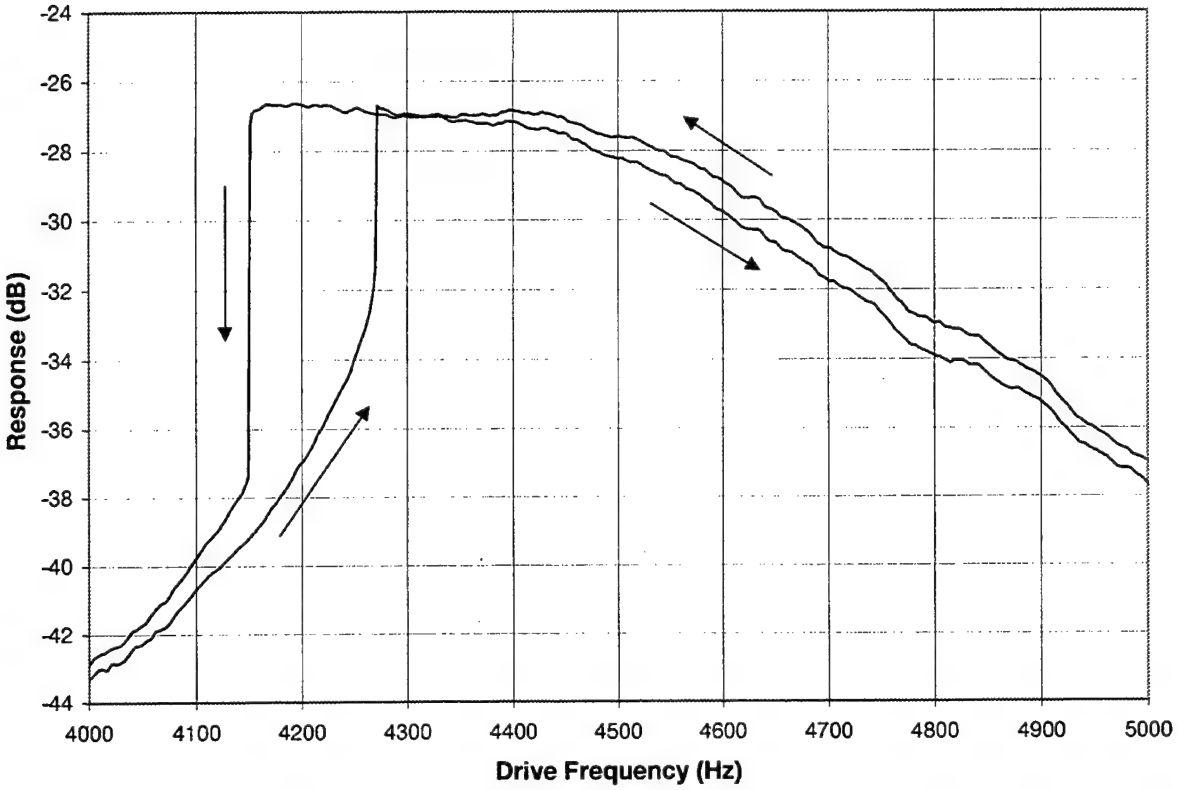

Figure 8.4. Frequency response (with the microphone) of the driver at 8.75 Vrms driving voltage

The last measurement consists of driving a pressurized test resonator with the assembled driver. The purpose is to measure the sound pressure response with a calibrated sensor and to determine if sufficiently high amplitudes can be achieved at elevated mean gas pressures. Also, the interaction of the piezoelectric disk resonance with the gas resonance can be

explored at elevated mean gas pressures. The last detail requires that the test resonator have an adjustable length to tune the gas resonance.

Unfortunately, not enough time was available to perform these tests with the piezoelectric driver.

IX. COST ANALYSIS AND COST ESTIMATE

This thesis presents a cost analysis of the mini TAR as a unique system, and evaluates its efficiency. This thesis will also compare the mini TAR with similar projects and determine which system best fits our requirements.

Cost analysis may be defined as an inquiry to assist decision makers in choosing preferred future courses of action by (1) systematically examining the relative objectives and the alternative policies or projects for achieving them; and (2) comparing quantitatively the economic costs, effectiveness (benefits), and risks of alternatives. (Fisher, 1975)

If there is more than one feasible system or option, cost analysis helps decision makers to determine which system is the most efficient. If only one system exists, (i.e., comparison of two or more options is impossible) cost analysis helps to assess whether or not the system is worth capital investment. Although both approaches could be used to perform a cost analysis of the mini TAR, the mini TAR's unique features distinguish it from other cooling devices, rendering the latter approach more effective.

In addition to the analysis of the mini TAR as a unique system, it should be noted that there are some commercial models that are similar to the mini TAR, and these models are basically used for the same purpose,

namely microchip cooling. Although functionally different, a comparison of these models may be useful for better decision-making.

A. COST ANALYSIS

This chapter is divided in two parts. The purpose of the first part is to perform a cost analysis of the mini TAR. The second part compares the mini TAR with the other existing refrigeration methods.

B. COST ANALYSIS AS A UNIQUE SYSTEM

The main objective for the cost analysis of the mini TAR is to develop and apply concepts and techniques for assessing the economic cost of the proposed or existing alternative future actions under conditions of uncertainty. In cost analysis, such alternative actions usually take the form of some combination of the following (Fisher, 1975):

- ***Proposed new capabilities for the future***
- ***Proposed modifications of existing or presently programmed capabilities***
- ***Proposed deletions from the presently planned force***
- ***Proposed combinations or packages of (1) through (3) – that is, total force structures for the future***

For the cost analysis of the mini TAR, the first option of proposed capabilities for the future is the best description. The areas in which the mini TAR will be used are very different than those of the traditional refrigeration devices (Fisher, 1975). Further information and a comparison of these devices with the mini TAR will be discussed later in this chapter.

Before defining the economic cost of the mini TAR, another significant aspect of cost analysis, which should be addressed, is the "life cycle" identification. This means that for a proposed new system (i.e., the mini TAR), provisions should be made for segregating the costs of the proposal into three cost categories:

Research and Development costs (R&D) – the resources required for developing the mini TAR to the point where it can be introduced into the operational inventory at some level of desired reliability.

Investment costs – the one-time outlays required to introduce the mini TAR into the operational inventory. This level also includes initial production and mass production costs.

Operating costs – the recurring outlays required year by year to operate and maintain the mini TAR in service over a period of years.

Since the mini TAR project is in its early stages of development, the only data available is about the research and development costs. For cost and benefit analysis, we need information about all life cycle levels, so

assumptions and predictions are made about the future costs of the mini TAR. Additionally, information about the investment and operating costs is obtained through comparisons of other similar projects.

The similarity of the projects may be defined in two different ways. It is possible to compare the mini TAR project with the functionally similar projects of other cooling devices, or with the projects that are functionally different but have similar life cycles. We will discuss the use of similar projects for analysis later in this chapter, and will start with the first step of life cycle cost analysis, R&D costs.

1. Research and Development Costs

The R&D expenses include labor, equipment, services and travel expenses. There are some expense subcategories. The expenditures detailed below cover only those incurred by the Naval Postgraduate School for this project. The expenditures of the Rockwell Company for its own research and development department are not included in this thesis.

The research and development costs of the mini TAR are listed as the NPS and the Rockwell. The present value of the research and development costs in NPS are listed below:

Labor	**$ 61.0 K**
Overhead (Travel)	
To Rockwell (3 trips for 2 per.)	$2.0 K
To onsite special fab.ser., Bay Area	$0.5 K
	$2.5 K
Equipment	
Data Acquisition software	$ 0.5 K
Piezoelectric transducer materials	$ 0.3 K
Pressure sensors for drivers	$ 2.5 K
Thin wall SS tubing & hemispheres	$ 0.5 K
Heat exchanger Ribbon	$ 2.9 K
Thermometry & Heater supplies	$ 0.7 K
Hand-held thermometers (3)	$ 1.4 K
Other consumables	$ 0.5 K
	$ 8.9 K
Services	
Laser welding	$ 1.2 K
Electroplating	$ 0.6 K
EDM Machining	$ 1.0 K
Conventional wel. & mach. (off-site)	$ 2.5 K
	$ 5.3 K
Grand Total	**$ 77.7 K**

Table 9.1. Research and Development Costs of the Mini TAR at NPS

Currently there is no information available about the R&D expenses for Rockwell. We assume that R&D will take three years, and for the first year (2000) the cost will be $30 K, and $100 K for the following two years. When inflation (around 3.5%) and discount rate (around 5%) are included, the present value (PV) of the R&D expenses is found using the following equation:

$$PV = \$\,30{,}000 + \frac{\$\,100{,}000}{(1+0.035+0.055)} + \frac{\$\,100{,}000}{(1+0.035+0.055)^2}$$

$$PV \cong \$\,30{,}000 + \$\,91{,}742 + \$\,84{,}168$$

$$PV \cong \$\,205{,}911 \cong \$\,206K$$

2. Investment Costs

The second part of the life cycle costs is the investment costs. Since we presently do not have any dollar values, assumptions and estimations are made about the investment costs. Because the mini TAR will most likely be manufactured by Rockwell (or another company that has existing labor and assembly lines), the investment costs will be relatively low. The manufacturer will mainly use existing capabilities by reallocating them and investing in additional capabilities if necessary. (Of course, reallocation is an additional expense, but building a new assembly line for the mini TAR will be

much more expensive.) The investment for the new assembly by reallocation is assumed to be around $50,000.

The investment costs include initial and mass production costs. We assume that for initial production level manufacturing, 100 mini TAR units are sufficient for the tests prior to mass production. In this level of life cycle, two different costs are the 100 test units and the cost of tests. If we assume the cost of the mini TAR during initial production to be around $800 for each unit, then the present value of the 100 mini TARs will be:

$$PV = \frac{M * \$ P}{(1 + \Omega + r)^N}$$

$$\begin{aligned} &M : Number\ of\ units \\ &P : \Pr ice\ of\ a\ unit \\ &\Omega : Inflation \\ &r : Interest\ rate \\ &N : Number\ of\ years \end{aligned} \qquad (9.1)$$

$$PV = \frac{100 * \$\,800}{(1 + 0.035 + 0.055)^3} \cong \$\,61{,}775$$

The second part of the expense of the initial production level is the cost of the tests. Although the details of those tests are not clarified, they will be about the performance, durability, and dependability of the mini TAR. The tests will be performed during the third year of the life cycle. If we expect the

cost of the tests to be $50,000 than we can calculate the present value o cost with Equation 9.1 as follows:

$$PV = \frac{\$\,50{,}000}{(1 + 0.035 + 0.055)^3} \cong \$\,38{,}609$$

After initial production level tests, the life cycle will proceed with the mass production level, assuming that the test results are satisfactory.

The mass production is assumed to begin at the beginning of the fourth year, and will continue for 10 years. We also assume that at least 5000 of the mini TAR units will be produced during the mass production level. This number may vary depending on the usage areas of the mini TAR and only represents a minimum.

During mass production, the cost of production will decrease to $300 per unit. The present value of cost of mass production can be calculated in two steps. First, the present value will be calculated, and then the projected value at the beginning of the fourth year. If we assume that the mass production is evenly distributed over ten years, and the cost of the production is adjusted for inflation, then we can calculate the present value of the cost of the mass production for 5000 units with the following equations:

$$FV = \frac{(M * \$\, P) * \left(1 - \frac{1}{(1+r)^N}\right)}{(r)}$$

(*Future value at the beginning of the fourth year*)

M : *Number of units* (9.2)

P : *Price of a unit*

r : *Interest rate*

N : *Number of years*

$$FV\,(at\ 2004) = \frac{(500 * \$\,300) * \left(1 - \frac{1}{(1+0.055)^{10}}\right)}{(0.055)} \cong \$\,1{,}130{,}643$$

The following equation is used to calculate the present value of the total mass production expenditures:

$$PV = \frac{C}{(1+r)^N}$$

C : *Cost* (9.3)

r : *Interest rate*

N : *Number of years*

$$PV = \frac{\$\,1{,}130{,}643}{(1+0.055)^4} \cong \$\,912{,}674$$

3. Operating Costs

Finally, the last part of the life cycle costs are the operating costs. Operating costs basically include the expenditures for maintaining and operating the system.

The mini TAR theoretically does not require any maintenance. However, in practice there may be some necessities for maintenance or more likely replacement, either because of a mistake during production or operation. In both cases, the probability of such an error is very low; however, it is not totally negligible in terms of cost. Although it might be much lower in reality, in this thesis production or operating errors are assumed to be around 1 %. Since the total cost of manufacturing 5000 mini TARs was $912,674, the total cost of replacements will be around $9,127.

The cost of energy consumed for operating the mini TAR is negligible, especially if we consider that the mini TARs will be used in systems like airplanes where the system produces its own power. The energy required by the mini TAR is very low when compared to the system resources, thus the cost of the energy becomes negligible.

However, there are some other costs, such as training and replacement, which may be analyzed under the category of operating costs. These costs are explained below.

Since the mini TAR does not need any human interface, it is reasonable to assert that extra training of the personnel may be unnecessary. The skills of the existing personnel will be sufficient to perform simple procedures such as the replacement of the unit or the performance checks. If we assume that some level of training is necessary, the cost of the training will be around $25000.

Replacement costs refers to the cost of replacing an old cooling system with a mini TAR. (Replacing a malfunctioning mini TAR with a new one is not analyzed under this category.) The replacement cost includes the cost of transferring the old system and replacing the new system. If the removed system can't be used somewhere else, the price of the old system is also included in the replacement costs. After replacement, the old system probably will not be used elsewhere, and is usually thrown away. This will increase the replacement cost, and as a result, the total life cycle costs increase.

Replacement is not necessarily an issue-- sometimes a system may be new and does not replace anything. Although there is not enough data available about the applications of the mini TAR, it is assumed that it will not replace an existing system. The mini TAR will most likely be a component that increases the capabilities of a new, larger system.

4. Decision Making and Benefits

The main objective of a cost analysis is to help decision makers t determine the extent to which investment in a particular project is beneficia or not. The easiest way to decide is to compare the relative value of costs and benefits. Basically, if benefits are more than the cost, the decision makers invest in the project. If there is more than one system, the decision makers will choose the project with the biggest benefit-cost difference.

However, benefit estimations are usually difficult because of the uncertainties of the metrics of benefits. For example, the mini TAR's unspecified applications are one uncertainty that makes cost estimation difficult. The mini TAR may be used in some airplanes under high temperature conditions, or on spacecrafts where there is no gravity and the ambient pressure is very low. But these are all predictions. It is not absolutely clear where the mini TARs are going to be used in the future, and some of the information regarding their planned usage is classified.

For the purposes of this thesis, we assume that the mini TAR is critical for some military or spacecraft equipment. However, caution must be taken before asserting that microchip cooling is a critical aspect of a revolutionary technological development, and the mini TAR is the only possible option. Such claims will bring us to the conclusion that money is not an issue, and

cost analysis is futile. It is too early to say that the mini TAR is the only option for high-tech airplanes or other devices, and there are some other systems available which could replace the mini TAR. A comparison of the mini TAR with other systems will be analyzed in the second part of this chapter.

Insufficient information about usage areas of the system and other uncertainties about benefits make cost analysis difficult. However, it is still possible to calculate the total cost and define this number as the baseline. If the perceived value of benefits surpass this line, than the project is feasible; otherwise, it is not.

The total cost of manufacturing 5000 mini TARs includes all of the costs mentioned above. The following table shows the total cost:

Research and Development Costs	
R&D by NPS	$ 77,700
R&D by Rockwell	$ 205,911
	$ 283,611
Investment Costs	
Assembly line	$ 50,000
Initial Production	$ 61,775
Tests	$ 50,000
Mass Production	$ 912,674
	$ 1,074,449
Operating Costs	
Maintenance and defective production	$ 9,127
Training	$ 25,000
	$ 34,127
Grand Total	**$ 1,392,187**

Table 9.2. The Overall Cost of Manufacturing 5000 Mini TARs

If the total cost of producing 5000 units of mini TARs is $1,392,187, then the cost of a mini TAR unit will be around $278. If the benefits of using a mini TAR in a particular system or project are more than $278, then we can conclude that investing in the mini TAR project is feasible and beneficial.

However, the mini TAR consumer will most likely be a government unit such as the U.S. Air Force, and the manufacturer is Rockwell, not a

governmental agency. Since Rockwell is a private and commercial company, it should earn profit. Rockwell will not sell mini TARs to the government for the actual cost. Since 30% is a reasonable average profit in the private sector, the price of the mini TARs for the U.S. Government would be approximately:

$$\begin{aligned} &P = (1 + 30\,\%) * C \\ &P : \mathrm{Price} \\ &C : Cost \end{aligned} \tag{9.4}$$

$$P = 1.3 * \$278 = \$\,361.4$$

Thus, the consumer will consider $361 as the reference level for decision-making. If the benefits are greater, then the user will buy the system.

Prior to making any final decisions, other considerations such as alternative investments must be taken into account, (i.e., the Air Force or the Rockwell can invest in other projects if the benefits are greater.) However, if the mini TAR project is crucial for national defense, or is determined to be irreplaceable, such a comparison may be irrelevant. Nevertheless, both the user and the manufacturer can look for other systems, which can replace mini TAR and maybe give better performance with less cost. The following paragraphs section compares the mini TAR with possible alternatives.

C. COST ANALYSIS WITH COMPARISON OF SIMILAR SYSTEMS

As mentioned at the beginning of this chapter, cost analysis can have two forms. It can be the comparison of the costs and benefits, or it can be the comparison of similar systems. The previous part of this chapter was interested in cost and benefit estimations. This next section will concentrate on the comparison of similar systems.

A comprehensive comparison of the mini TARs with other cooling systems is difficult, since it is not clear where and how they will be used. But, if we focus on the main function of the mini TAR, which is cooling microchips, we can find some similar systems.

The most common cooling system is the cooling fan. Cooling fans are used in most of the personal computers and some electronic equipment. Although the function of the cooling fans resembles to the purpose of the mini TAR, there are differences. First, the mini TAR as mentioned in chapter 3 is supposed operate between 60°C and 90°. Fans may not provide cooling if the ambient air temperature is too hot. Second, the mini TAR may be used for the devices where vibration is not wanted. Fans generate vibration. Finally, the mini TAR can operate anywhere. However, fans need air for cooling.

Another possible alternative may be heat pipes. The general principle of the heat pipes is similar to standard refrigerators. The evaporation of the

liquid into a gas absorbs heat causing the environment to become cooler. However, since heat pipes are highly sensitive to gravity and stability, they are useless on moving platforms like airplanes or satellites.

For cost analysis and comparison purposes, these first two options are not practical. Although the functions appear similar, the capabilities and the usage areas of the systems are totally different.

Another option is thermoelectric coolers, which are solid state devices. These have cooling efficiencies that are modest but adequate for many purposes. The maximum operating temperature of these devices is about 80°C, which effectively eliminates them from consideration. These devices are also susceptible to damage from large vibrations and absorption of moisture, although these failure mechanisms could be resolved by proper hardware design.

The last alternative, also studied by the Rockwell research and development division, is the injection of liquid refrigerant onto the surface of the device being cooled. The cooling process is similar to a heat pipe, except that active transport of the refrigerant is provided, and gravity and accelerations do not affect the performance. The information related to this technology is classified, and further information is too limited for further discussion. However, the project is the most similar alternative of the mini TAR, and is a logical object for comparison.

However, there are two more problems that may affect the effectiveness of a comparison between the mini TAR and the refrigerant injection. First, it is still not clear whether or not the refrigerant injection will work, and second, there is no information available about the costs of the system. If in the future both systems satisfy the requirements, then it may be worthwhile to perform a more extensive comparison of each method's advantages and disadvantages.

X. CONCLUSIONS

A. THERMOACOUSTIC REFRIGERATION

Thermoacoustic refrigeration is a relatively new concept in refrigeration technology. Although thermoacoustic experiments have been performed for the last 15 years, actual usage of thermoacoustic refrigerators (TAR) in technology has yet to be applied.

There are some reasons why TARs are impractical. First of all, they are not as efficient as traditional refrigerators in terms of energy consumption. Although there have been some experimental improvements, the TAR's cooling efficiency is still below acceptable limits, particularly since the efficiency of traditional refrigeration continues to improve. Secondly, TARs are not cost effective when compared with other cooling systems until mass-production costs can be achieved. And finally, since the technology is new, current TARs do not satisfy the performance requirements defined by Rockwell. Technological equipment may require greater cooling capacity than that of existing TARs.

Nevertheless, there may be some exceptions in which the benefits of using a TAR surpass those of other systems. TAR technology may be superior to either traditional vapor-compression refrigeration or Stirling refrigeration in the context of miniature devices spanning modest temperature differences.

Miniaturization is likely to be too difficult for vapor-compression or Stirling technologies.

Also, TARs may have some advantages in satellites or high-speed aircraft. There are also specific contexts in which the TAR is the only feasible refrigeration option, wherein other systems would be incompatible. Hot environments preclude the use of current thermoelectric devices.

Internationally, scientists are making efforts to improve TARs. The experimental results show promising potential for the future of this new technology.

B. THE MINI TAR

The mini TAR is one of the newest practical applications of the TARs, and is thus named due to its small size. All thermoacoustic laws apply to mini TARS as well as to any other TAR. Currently there are no TARs, which are being used in a system or commercially tested. In the near future it may be possible to see mini TARs installed on high-tech military instruments. The application of mini TAR in civilian technology may take longer because of the high cost of this new technology or its unfamiliarity.

C. THIS THESIS AND FURTHER EFFORTS

The goal of this thesis is to design and develop a mini TAR fulfilling the requirements outlined in Chapter 6; and to assess its cost-benefit characteristics. The design of the new TAR, while similar to the previous designs, is more complex due to its smaller size.

Contrary to the previous TAR models, the mini TAR has unique small parts, which are not easily acquired. Almost all of the parts are designed and manufactured by Naval Postgraduate School personnel in Monterey, California. Even the piezo disk, which was originally manufactured by Motorola, has been modified significantly so it could be used in the driver unit.

The mini TAR has two main units, the driver and the resonator. Although temporary resonators were used for measurements, this thesis is focused on the driver unit. The objective was to obtain maximum performance from the driver.

In terms of performance, the resonator is equally as important as the driver. The properties of the stack and the gas inside the resonator tube are crucial parameters, as are those of the resonator. Further research efforts on the resonator should concentrate on these variables and increasing the overall performance of the mini TAR.

In summary, the basic piezoelectric flexural disk was found to have very good displacement and power capabilities at its nominal resonant frequency. The estimated values are a peak displacement of at least 38 μm, a vibration power of at least 1 W, and an operating frequency of about 4 kHz for a single disk.

While the resonant frequency of the piezo disk did vary considerably with respect to differences in the disk-mounting configuration, this was expected. However, resonant frequency changes were also observed with a fixed configuration coupled to an acoustic resonator, when the drive amplitude was varied. This was surprising and the frequency changes were as large as 2 %.

While the stainless steel diaphragm works acceptably well to couple the piezo disk motion to the acoustic resonator, this component is currently limiting the acoustic power level to a value significantly less than the capability of the piezo disk. Improvements to the design of the diaphragm could be very valuable.

In terms of cost-benefit analysis, improvements in the manufacturing process of the Mini TAR could signal new and wider usage in aerospace, industrial and maybe even home applications.

LIST OF REFERENCES

1. Swift, G.W., "Thermoacoustic Engines and Refrigerators", Physics Today, pp. 22-28, July 1995.

2. Purdy, E.W., "Development of a Graphical Numerical Simulation for Thermoacoustic Research", December 1998.

3. Wheatley, J.C., Swift, G.W., and Migliori, A., "The Natural Heat Engine", Los Alamos Science, number 14, pp. 2-29, Fall 1996.

4. Moran, M.J., Shapiro, H.N., Fundamentals of Engineering Thermodynamics, John Wiley and Sons, 1988.

5. Swift, G.W., "Thermoacoustic Engines", Journal of the Acoustical Society of America, v.84, p. 1145-1179, 1988.

6. Wong, K., "Solving Ordinary Differential Equations with Runge-Kutta Methods", June 1996, [www.geog.ubc,ca/numeric/labs/lab4/lab4/lab4.html].

7. Kreyszig, E, Advanced Engineering Mathematics, 6th ed, John Wiley and Sons, 1988.

8. Allen, R.C., Avery, P., and Wallace, J.Y., "Lower/Upper Triangular (LU) Decomposition", Computational Science Textbook, Sandia Corporation, 1998, [ais.cs.sandia.gov/AiS/textbook/textbook.html].

THIS PAGE INTENTIONALLY LEFT BLANK

INITIAL DISTRIBUTION LIST

1.	Defense Technical Information Center 8725 John J. Kingman Rd., STE 0944 Ft. Belvoir, VA 22060-6218	2
2.	Dudley Knox Library Naval Postgraduate School 411 Dyer Rd. Monterey, CA 93943-5001	2
3.	Professor T. Hofler, Code PH/HF Naval Postgraduate School Monterey, CA 93943-5001	4
4.	Professor Roger Evered, Code SM/RE Naval Postgraduate School Monterey, CA 93943-5001	3
5.	Turkish Navy Headquartes DzKK Bakanliklar Ankara-Turkey	1
6.	LTJG Omer Livvarcin 376 F. Bergin Dr. Monterey, CA 93940	1
7.	Jeffrey F. Denatale Mail Stop A23 1049 Camino Dos Rios Thousand Oaks, CA 91360	1
8.	C. L. Chen Mail Stop A35 1049 Camino Dos Rios Thousand Oaks, CA 91360	1